Developmental Biology **251,** 221–240 (2002)
doi:10.1006/dbio.2002.0828

Properties of a Fetal Multipotent Neural Stem Cell (NEP Cell)

Jingli Cai,*,† Yuanyuan Wu,† Takumi Mirua,* Jeanne L. Pierce,‡ Mary T. Lucero,§ Kurt H. Albertine,† Gerald J. Spangrude,‡ and Mahendra S. Rao*,†,[1]

**Laboratory of Neurosciences, National Institute on Aging, Baltimore, Maryland 21224; and Departments of †Neurobiology and Anatomy, ‡Oncological Sciences, and §Physiology, University of Utah, Salt Lake City, Utah 84132*

Multipotent neural stem cells (NSCs) present in the developing neural tube (E10.5, neuroepithelial cells; NEP) were examined for the expression of candidate stem cell markers, and the expression of these markers was compared with later appearing precursor cells (E14.5) that can be distinguished by the expression of embryonic neural cell adhesion molecule (E-NCAM) and A2B5. NEP cells possess gap junctions, express connexins, and appear to lack long cilia. Most candidate markers, including Nestin, Presenilin, Notch, and Numb, were expressed by both NEP cells as well as other cell populations. Fibroblast growth factor receptor 4 (FGFR4), Frizzled 9 (Fz9), and SRY box-containing gene 2 (Sox2) as assessed by immunocytochemistry and *in situ* hybridization are markers that appear to distinguish NSCs from other precursor cells. Neither Hoechst 33342 nor rhodamine-123 staining, telomerase (Tert) expression, telomerase activity, or breakpoint cluster region protein 1 (Bcrp1) transporter expression could be used to distinguish NEP stem cells from other dividing cells. NEP cells, however, lacked expression of several lineage markers that are expressed by later appearing cells. These included absence of expression of CD44, E-NCAM, A2B5, epidermal growth factor receptor (EGFR), and platelet-derived growth factor receptor-alpha (PDGFRα), suggesting that negative selection using cell surface epitopes could be used to isolate stem cell populations from mixed cultures of cells. Using mixed cultures of cells isolated from E14.5 stage embryos, we show that NEP cells can be enriched by depleting differentiating cells that express E-NCAM or A2B5 immunoreactivity. Overall, our results show that a spectrum of markers used in combination can reliably distinguish multipotent NSCs from other precursor cells as well as differentiated cells present in the CNS.

Key Words: **NSC; NEP; NRP; GRP; differentiation; precursor.**

INTRODUCTION

The early-formed neural tube (at E10.5 in rats) consists of proliferating, morphologically homogeneous cells termed NEP stem cells (Kalyani *et al.,* 1997). NEP cells can be maintained in culture and undergo self-renewal, and single NEP cells can differentiate into neurons, astrocytes, and oligodendrocytes (Kalyani *et al.,* 1997, Mujtaba *et al.,* 1999). Thus, NEP cells represent one of the earliest identifiable NSC populations. The fetal NSC (NEP cell) is thought to generate all the differentiated cells of the CNS via the generation of intermediate precursors that arise from stem cells, by a process of symmetric and asymmetric divisions. The intermediate precursors migrate away from the ventricular zone (reviewed in Panicker and Rao, 2000) and ultimately generate fully differentiated cells. We have identified two such intermediate restricted precursors (neuronal restricted and glial restricted precursors; NRP and GRP, respectively) and have also demonstrated a direct lineage relationship between NEP cells and these more restricted cells (Mayer-Proschel *et al.,* 1997; Rao and Mayer-Proschel, 1997). These partially differentiated precursor cells begin to express differentiation markers, such as E-NCAM and A2B5, while migrating from the ventricular zone and can be distinguished from stem cells both functionally and antigenically (reviewed in Rao, 1999). At E14.5, approximately 60% of the cells express E-NCAM and 30% of the cells

[1] To whom correspondence should be addressed. Fax: (410) 558-8323. E-mail: Raomah@grc.nia.nih.gov.

0012-1606/02 $35.00

express A2B5, while 10% of the cells present primarily in the ventricular zone lack the expression of E-NCAM or A2B5.

As development proceeds, the ventricular zone becomes significantly diminished in size and the number of NSCs that can be harvested is significantly reduced (unpublished results). The properties of NSCs are altered as well. Notably, EGFR expression is upregulated and stem cells begin to respond to EGF by increasing proliferation (Reynolds *et al.*, 1992; Reynolds and Weiss, 1996). EGF/FGF-dependent multipotent NSCs continue to be present throughout the rostrocaudal axis throughout development, and while their exact location in the adult is unclear, cells can be harvested from multiple regions in adults (Reynolds *et al.*, 1992; Santa-Olalla and Covarrubias, 1995). After E14.5, NSCs have been cultured in the form of neurospheres in suspension culture in high concentrations of FGF or EGF, where the stem cell population consists of a small subset of the total number of cells present within the neurosphere. Later appearing NSCs can be distinguished from NEP cells primarily by the absence of EGFR expression and lack of a proliferative response to EGF by NEP cells (Kalyani *et al.*, 1999).

The inability to localize NSCs *in vivo* except at early developmental stages (NEP cell stage) and the inability to obtain a purified population of NSCs have made characterizing the properties of NSCs difficult. Controversy exists as to growth factor response, antigenic expression, differentiation potential, alteration of phenotype in culture, and lineage relationship with other precursors. Furthermore, in the absence of a purified population of NSCs, it has been difficult to assess properties that might be universal to all NSC populations, such as Hoechst 33342 efflux (Goodell *et al.*, 1996), rhodamine-123 fluorescence (Leemhuis *et al.*, 1996; Radley *et al.*, 1999; Hulspas and Quesenberry, 2000), telomerase levels (Kruk *et al.*, 1996), and forward vs side scatter properties (McLaren *et al.*, 2001).

In this manuscript, we have taken advantage of our observation that a pure population of fetal NSCs (NEP cells) can be isolated from rat E10.5 neural tubes to examine their properties and the expression of candidate stem cell markers in detail. We have compared their properties with those of later appearing precursor populations (NRP and GRP cells). We demonstrate that NEP stem cells can be distinguished from other cells by the presence of FGFR4, Sox2, and Fz9 and by the absence of several early differentiation markers. We also show that several other markers that have been used, as markers of stem cells, are not unique to stem cells but are also expressed by more restricted precursor cells. We show that telomerase levels and efflux of the fluorescent dyes rhodamine-123 and Hoechst 33342 cannot be used to distinguish NEP cells from other precursor cells. We show, however, that NEP cells can be reliably distinguished from other dividing populations of cells by the absence of expression lineage-specific markers that include E-NCAM and A2B5.

MATERIALS AND METHODS

Animal Experimentation

All experiments involving use of animals were approved by the IUAUC at the NIA. Animals were maintained in an approved animal facility until required for the experiments. Animals were sacrificed by using CO_2 inhalation as recommended by the IUAUC. All experiments, unless otherwise stated in Results, were performed at least three times.

Isolation of NEP Cells, E14.5 Neural Tube Cells, and GRP Cells

Sprague–Dawley rat embryos (Harlan) were removed from timed-pregnant rats at 10.5 or 14.5 gestation day as described (Wu *et al.*, 2002). To get NEP cells, the trunk segments of the E10.5 embryos were dissected and incubated in an enzyme solution containing Collagenase type I (1 mg/ml; Worthington Biochemical) and Dispase II (2 mg/ml; Roche) in Ca^{2+}/Mg^{2+}-free Hank's balanced salt solution (Gibco/BRL), at room temperature for approximately 10 min. The enzyme solution was then replaced by NEP basal medium (Kalyani *et al.*, 1997) with 10% chicken embryo extract (CEE). The segments were gently triturated with a Pasteur pipette (Fisher) to release neural tubes from surrounding somites and connective tissue. Isolated neural tubes were dissociated by Trypsin–EDTA, and NEP cells were grown in NEP basal medium with 10% CEE.

To obtain E14.5 neural tube cells or GRP cells, neural tubes were mechanically dissected from E14.5 embryos. Isolated neural tubes were dissociated by Trypsin–EDTA, and E14.5 cells were grown in NEP basal medium. GRP cells were obtained by sorting the A2B5-positive cells from E14.5 neural tube cells (sorting details are as described below).

Cultures of Rat NEP Cells and E14.5 Neural Tube Cells

Tissue culture dishes were coated with fibronectin (Sigma), which was diluted to a concentration of 20 μg/ml in distilled H_2O (Sigma), for a minimum of 4 h. Poly-L-Lysine (PLL)/laminin double-coated dishes were prepared by first coating with PLL (30–70 kDa; Sigma; dissolved in distilled water at a concentration of 13.3 μg/ml) for 1 h, followed by incubation with laminin (Biomedical Technologies Inc.; dissolved in distilled water at a concentration of 15 μg/ml) overnight at 4°C. Excess laminin was discarded, and the dishes were rinsed with medium just prior to use. Acutely dissected or sorted NEP cells were plated on a fibronectin-coated 60-mm dish (Corning) and maintained at 37°C, 5% CO_2 in NEP-basal medium with 10% CEE and basic fibroblast growth factor (bFGF, 30 ng/ml; Peprotech). Acutely dissected or sorted E14.5 neural tube cells were plated on PLL/Laminin-coated dishes and maintained at 37°C, 5% CO_2 in NEP-basal medium with bFGF (20 ng/ml).

Electron Microscopy

Neural tubes were prepared for light microscopy, transmission electron microscopy (TEM), and low-vacuum scanning electron microscopy (SEM). Briefly, neural tubes were dissected from rat embryos at E10.5 and E14.5, immersed in 2.5% glutaraldehyde/1% paraformaldehyde in cacodylate buffer for 12 h (pH 7.4, 310 mOsm/kg H_2O, 4°C), and postfixed in 2% osmium tetroxide for

TABLE 1
PCR Primers

Gene	Product size (bp)	Sequence (Sense and Antisense)
Bcrp1	327	5′-CCA TAG CCACAG GCC AAA GT-3′
		5′-GGG CCA CAT GAT TCT TCC AC-3′
Brn1	450	5′-CAA CAG CCA CGA CCC TCA CT-3′
		5′-CAG AAC CAG ACC CGC ACG AC-3′
Cx43	291	5′-TAC CAC GCC ACC ACT GGC CCA-3′
		5′-ATT CTG GTT GTC GTC GGG GAA ATC-3′
Cx45	1227	5′-GGG CAA ACC AAT TCC ACC ACC-3′
		5′-CAA GAT TAA ATC CAG ACG GAG-3′
EGFR	205	5′-GCT GGG GAA GAG GAG AGG AGA-3′
		5′-ACG AGT GGT GGG CAG GTG TCT T-3′
FGFR4	297	5′-TCC GAC AAG GAT TTG GCA G-3′
		5′-GCA CTT CCG AGA CTC CAG ATA C-3′
G3PDH	758	5′-TGA TGG GTG TGA ACC ACG AG-3′
		5′-CTC CTG TTG TTA TGG GGT CTG-3′
GFAP	388	5′-GAA ACC AAC CTG AGG CTG GAG-3′
		5′-GGC GAT AGT CAT TAG CCT CG-3′
Hes1	307	5′-CAC GCT CGG GTC TGT GCT GAG AGC-3′
		5′-ATG CCA GCT GAT ATA ATG GAG-3′
Hes5	244	5′-GTG GAG ATG CTC AGT CCC AAG-3′
		5′-TGT AGT CCT GGT GCA GGC TC-3′
Musashil	213	5′-CTA TCC CTC TCA CGG CTT ATG-3′
		5′-CGC TGA TGT AAC TGC TGA CC-3′
Nestin	317	5′-AGT GTG AAG GCA AAG ATA GC-3′
		5′-TCT GTC AGG ATT GGG ATG GG-3′
NF	186	5′-GCC GAG CAG AAC AAG GAG GCC ATT-3′
		5′-CTG GAT GGT GTC CTG GTA GCT GCT-3′
Notch1	976	5′-TCA AGG CCC GGA GGA AGA AGT C-3′
		5′-TCA GGG GAT GGG GTG AGG AAG-3′
Numb	460	5′-AAC AAT CCC CAT GCT ATC CCA CG-3′
		5′-GCT GCT GGG CCC GCA CAC TC-3′
PDGFRα	331	5′-CTG TAA CTG GCA GGC TCG GAG-3′
		5′-GTT GTC TGC AGT ACA AGT TGG CG-3′
PLP/DM20	515	5′-GAC ATG AAG CTC TCA CTG GCA C-3′
		5′-CAT ACA TTC TGG CAT CAG CGC-3′
Prominin	361	5′-GGA CAA AAC AGG AAG GAA GAG C-3′
		5′-TGG AGG AGA GGT TAC TGG TGA G-3′
PS1	233	5′-AGC GAT GAT GGT GGC TTC AG-3′
		5′-ATG GTT GTG TTC CAG TCC CC-3′
PS2	443	5′-ATC CTC ATT GGC TTG TGT CTC-3′
		5′-CCT CAT CCC TGA AGA TAG GC-3′
Tert	185	5′-GAC ATG GAG AAC AAG CTG TTT GC-3′
		5′-ACA GGG AAG TTC ACC ACT GTC-3′

2 h. For light microscopy and TEM, the fixed neural tubes were dehydrated in a graded acetone series, embedded in epoxy resin, and cut in cross-section (Albertine *et al.*, 1999). Thick sections (0.5 μm) were stained with 1% toluidene blue and photographed by using a Zeiss Axiophot brightfield microscope equipped with a Jenoptik ProgRes 3012 color digital camera (Jena). The color digital images were 4608 × 3480 pixels, at a resolution of 600 dpi. Thin sections (80 nm) were cut by using a Diatome diamond knife and counterstained with uranyl acetate and lead citrate. We used a Hitachi H-7100 transmission electron microscope to observe and photograph the thin sections, using conventional TEM film. For SEM, the osmicated neural tubes were rinsed in cacodylate buffer, cut in cross-section, and placed in distilled water (Garat *et al.*, 1996). We placed the moist neural tubes in a Hitachi S2460-N low-vacuum SEM. The neural tubes were not critical point dried or sputter-coated. Specimen chamber pressure was 25 Pa, accelerating voltage was 25 kV, and beam current was 250 microamps. Imaging of the moist, uncoated specimens was done by using a Robinson back-scatter detector. The digital images were 2048 × 1536 pixels, at a resolution of 450 dpi.

PCR Primers and Amplification

RNA isolation and cDNA synthesis. Total RNA was isolated directly from freshly dissected E10.5 and E14.5 neural tubes with TRIzol (Gibco/BRL), a modification of the guanidine

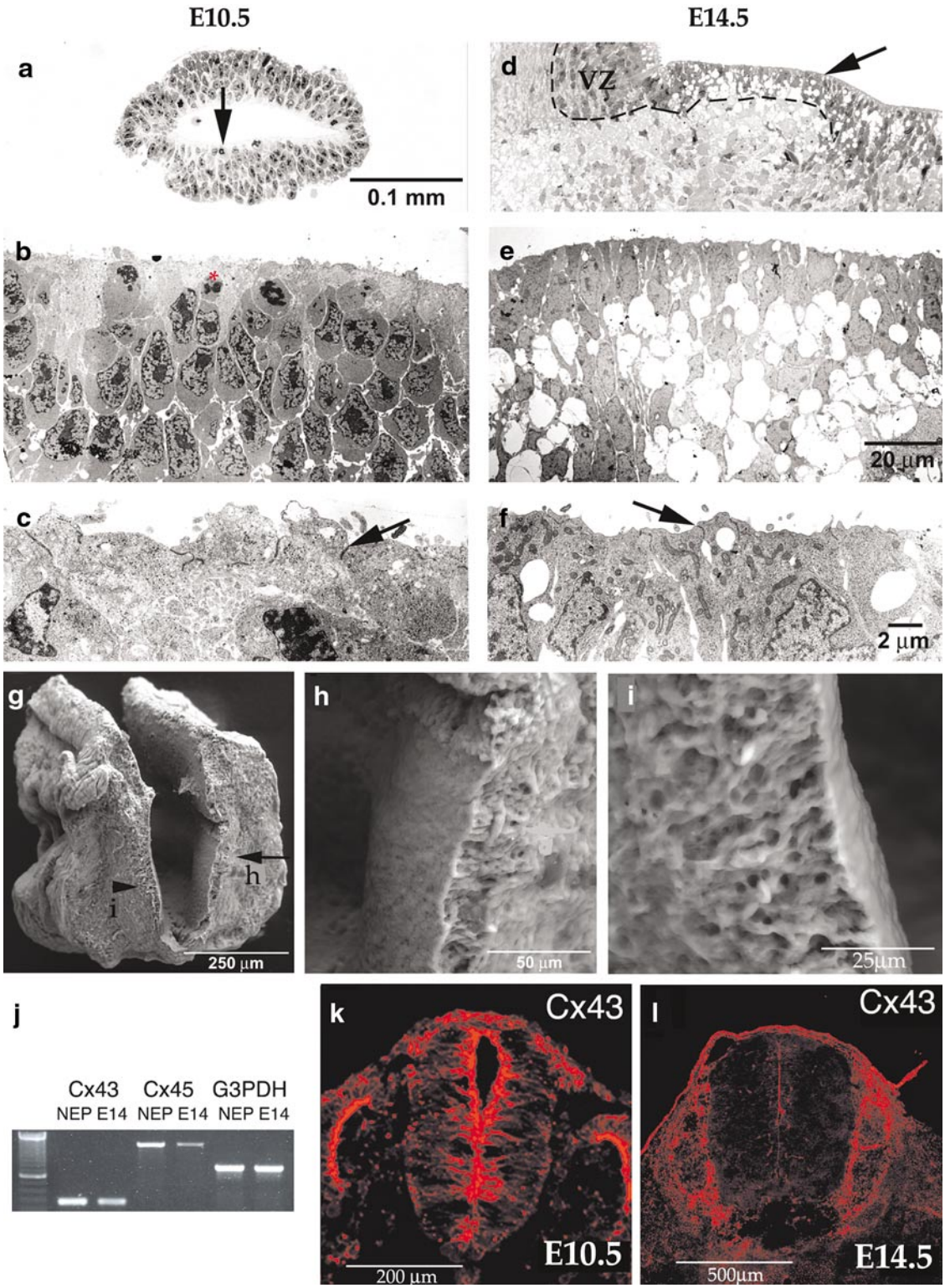

FIG. 1. Histologic and ultrastructural appearance of neural tubes dissected from rats at E10.5 and E14.5. The histologic areas indicated by the arrow in (a) and (d) are shown in corresponding electron micrographs (b and c, e and f, respectively). The luminal surface lacks microvilli and cilia. Luminal NEP cells are attached to adjacent cells by junctions (arrows in c and f). At E10.5 (b and c), the neural tube epithelial cells are oval to circular in shape, their cytoplasm contains few organelles, and their nuclei contain prominent nucleoli. Mitotic figures are

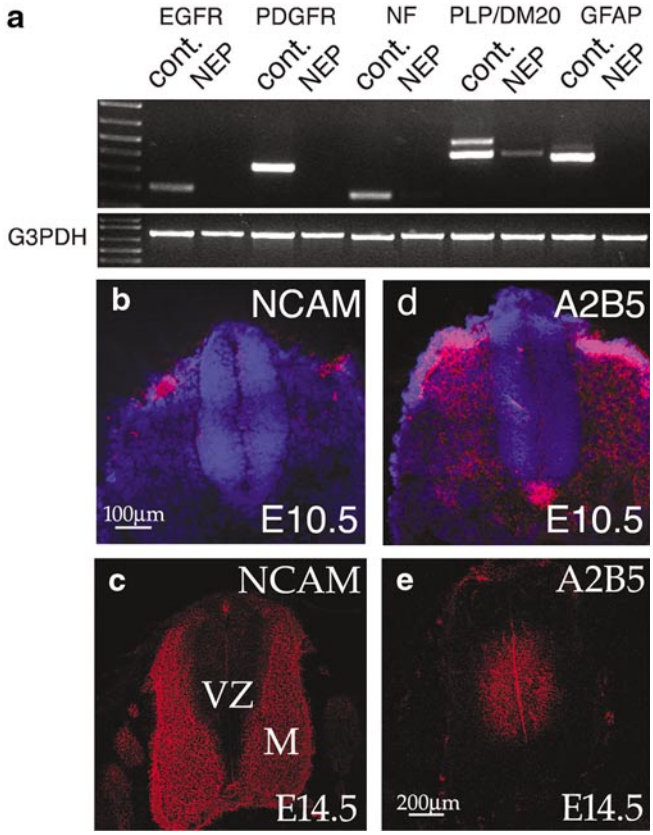

FIG. 2. NEP cells do not express early markers of differentiation. Neural tubes were dissected at E10.5 and processed for RT-PCR (a) or immunocytochemistry (b–e). Primers used were tested for specificity, and samples were run in duplicate. Levels of expression were estimated by normalizing levels with the expression of G3PDH. Experiments were repeated with independent isolations of samples at least three times. (a) NEP cells do not express EGFR, PDGFRα, NF, PLP/DM20, and GFAP, while bands were detected in the positive control samples. Note the trace expression of DM20, but not PLP at E10.5, suggesting an early onset of expression of this marker. (b–e) Cryostat sections from fresh frozen embryos (E10.5 and E14.5) were stained with E-NCAM (red, b and c) and A2B5 (red, d and e), and counterstained with DAPI (blue, in b and d). Neither E-NCAM (c) nor A2B5 (e) immunoactivity was seen at E10.5. E-NCAM was expressed in the mantle part (marked as M), which was outside of ventricular zone (marked as VZ) at E14.5 neural tube (b), and A2B5 was expressed in a restricted ventral domain (d) that overlaps with the known expression of other glial markers (Liu *et al.*, 2002).

isothiocyanate-phenol-chloroform extraction method. cDNA was synthesized by using 100 ng total RNA in a 20-μl reaction with Superscript II (Gibco/BRL) and oligo $(dT)_{12-18}$ (Gibco/BRL). One microliter of RNase H (Gibco/BRL) was added to each reaction tube, and the tubes were incubated for 20 min at 37°C before proceeding to the RT-PCR analysis.

PCR primers. PCR primers are listed in Table 1.

PCR amplification. A 0.5-μl cDNA template was used in a 50-μl reaction volume with the RedTaq DNA polymerase (Sigma). The cycling parameters were: 94°C, 1 min; 55°C, 1 min; 72°C, 1 min, for 30 cycles. The PCR cycles were preceded by an initial denaturation of 3 min at 94°C and followed by a final extension of 10 min at 72°C.

Immunocytochemistry

Staining procedures were done as described previously (Rao and Mayer-Proschel, 1997). Rat embryos were harvested, and either fresh frozen or fixed embryos (4% paraformaldehyde overnight) were sectioned at 12 μm on a cryostat (Leica). These sections were processed for immunocytochemistry as described below. Staining for the cell surface markers, such as A2B5, E-NCAM, and GalC, was carried out in cultures of living cells without permeabilization. To stain cells with antibodies against cytoplasmic antigens, cultures were fixed with 2% formaldehyde for 30 min at room temperature. In general, cultured cells or sections were incubated with primary antibody overnight at 4°C, followed by incubation with an appropriate secondary antibody at room temperature for 30 min. Double-labeling experiments were performed by simultaneously incubating cells in appropriate combinations of primary antibodies followed by non-cross-reactive secondary antibodies. Bisbenzimide DAPI (Sigma) histochemistry was performed as described previously (Kalyani *et al.*, 1997). Bisbenzimide staining was generally done after labeling had been completed. E-NCAM and Nestin antibodies were hybridoma supernatants obtained from Developmental Studies Hybridoma Bank (DSHB) and used at a 1:5 dilution. The A2B5 antibody was obtained from ATCC. β-III tubulin antibody (1:500; Sigma), GalC antibody (1:5; a kind gift from Dr. Ranscht), and GFAP antibody (1:500; Dako) were used as described previously (Rao and Mayer-Proschel, 1997). Antibodies to presenilin1 (PS1) were a gift from Dr. Mark Mattson (National Institute on Aging) and were used at a 1:50 dilution. Anti-Cx43 antibodies were purchased from Chemicon and used at a 1:250 dilution. Sox2 antibodies were obtained from Dr. Pevny and were used at a 1:2000 dilution.

Brdu Incorporation

To assess the proliferation of neural cells, 5-bromo-2′-deoxyuridine (10 μM) (Brdu; Sigma) was added to the cells for 6 h. The cells were then fixed with 2% paraformaldehyde for 30 min at room

prevalent (one sample is indicated by * in b). At E14.5 (e and f), the neural tube epithelial cells are more elongated, their cytoplasm contains numerous mitochondria and rough endoplasmic reticulum, and their nuclei display few nucleoli. Vacuoles are present, which appeared while the neural tubes were dissected. Low-vacuum SEM appearance of neural tubes dissected from mice at E14.5 (g–i). (g) is a survey view. The arrows in (g) identify the areas that are shown at higher power in (h) and (i). The luminal surface lacks microvilli and cilia. RT-PCR amplification of Cx43 and Cx45 messages shows both NEP cells and E14.5 cells express these two components of gap junction, while levels are decreased at E14.5 (j). Anti-Cx43 antibody was used to examine protein expression in the sections of E10.5 and E14.5 neural tube (k and l). Cx43 was downregulated and was almost undetectable at E14.5.

temperature. Cells were washed three times with PBS containing 5% goat serum and permeabilized with 2 M HCl for 10 min. Acid was removed by three washes with PBS containing 5% goat serum, and the residual HCl was neutralized with 0.1 M sodium borate (Sigma) for 10 min. After rinsing with PBS, cells were incubated with rat anti-Brdu antibody (1:10; Accurate) at 4°C overnight in buffer containing 0.5% Triton X-100. The cells were then incubated with goat anti-rat IgG (1:100; Jackson ImmunoResearch) for 30 min. After three washes with PBS, cells were observed under a Zeiss Fluorescence microscope and images obtained on a Zeiss digital camera.

Intracellular Ca^{2+} Measurements

Calcium imaging experiments were performed on rat NEP cells, which were acquired as above and plated on 25-mm round glass coverslips. Cells were loaded with 5 μM fura-2 AM and 80 μg/ml pluronic F127 (Grynkiewicz *et al.,* 1985) in rat Ringer's (RR) composed of (in mM): 140 NaCl, 3 KCl, $MgCl_2$, 2 $CaCl_2$, 10 Hepes, and 10 glucose and set to pH 7.4 with NaOH, for 1 h at 23°C in the dark. The cells were then washed three times with RR, and the fura-2 was allowed to de-esterify for 30 min. Changes in the ratio of fluorescence emission intensity at 520 nm by excitation at 340/380 nm were measured and correlated to changes in intracellular calcium, $[Ca^{2+}]_i$, using a standard two-point calibration scheme (Grynkiewicz *et al.,* 1985).

A Zeiss–Attofluor imaging system (Atto Instruments Inc.) was used to acquire and analyze the data, which were sampled at 1 Hz. Data were collected from a square region of interest (ROI) over the center of each cell. Cells were constantly perfused at 1–1.5 ml/min with RR. Neurotransmitters were made fresh in RR and delivered by bath exchange using a small volume loop injector (200 μl) located approximately 250 μl upstream from the bath. A response to neurotransmitter was defined as a minimum 10% transient rise over the baseline fluorescence ratio within 20 s from the time of loop insertion. The dead time from loop to bath in port was approximately 10–15 s. Neurotransmitters examined included: γ-aminobutyric acid (GABA), glutamate (E), and acetylcholine (ACh), all at 500 μM, and 100 nM pituitary adenylate cyclase activating peptide (PACAP). In addition, a 50-mM K^+ RR solution was used to depolarize the cells and to test for Ca^{2+} influx through voltage-gated channels (45 mM NaCl in RR replaced by 45 mM KCl). Control applications of RR had no effect. The pH of all test solutions was adjusted to 7.4 with 1 M NaOH.

In Situ Hybridization

Anti-sense RNA probes were generated by *in vitro* transcription (T3–T7 MaxiScipt Kit; Ambion), and labeled with digoxigenin-11-UTP (Roche). Mouse embryos were hybridized with FGFR4 anti-sense probe made from 2487 bp to 3077 bp of FGFR4 (NM_008011) and with Fz9 anti-sense probe obtained from the 0.3-kb 3′ UTR of Fz9 (Van Raay *et al.*, 2001). Paraffin sections (20 μm) were cut from stained embryos.

Hoechst 33342 and Rhodamine-123 Labeling and Flow Cytometry Assay

Cells were dissociated from freshly dissected E10.5 and E14.5 neural tubes and resuspended to 2×10^5 cells/ml in cell culture medium. Cells were incubated at 37°C in 5% CO_2 in the presence of 1 μM Hoechst 33342 (Molecular Probes) for 60 min. After washing with medium to eliminate residual dye, cells were again incubated at 37°C in 5% CO_2 for another 20 min. Cells were maintained at 4°C in PBS containing 5% fetal bovine serum (Gibco/BRL) for sorting and stained with 1 μg/ml propidium iodide (PI; Molecular Probes) just prior to sorting.

For rhodamine-123, labeling cells were incubated at 37°C in 5% CO_2 in the presence of 200 ng/ml rhodamine-123 (Molecular Probes) for 20 min. After incubation, cells were maintained on ice in PBS with 5% serum as described for Hoechst 33342 staining.

Flow cytometric analysis was performed with a FACS Vantage flow cytometer (Becton Dickenson Immunocytometry Systems). Then, 1×10^5 stained cells were analyzed for each staining. The cells were excited at 488 nm for Rhodamine 123 or PI and at 350 nm for Hoechst 33342. Hoechst emissions were monitored at 450 and 675 nm to assess the presence of a "side population" as previously described (Goodell *et al.,* 1996). The histograms of the Hoechst 33342 and rhodamine-123-positive cell population and two-dimensional dot graphs were plotted with CellQuest software (Becton Dickenson Immunocytometry Systems).

Assessing Telomerase Activity Levels

NEP cells and E14.5 neural tube cells were obtained from freshly dissected rat E10.5 and E14.5 neural tubes. Cells from other stages were obtained from acutely dissected neural tubes from rat embryos. GRP cells were isolated from E14.5 mixed culture sorted by flow cytometry with A2B5 immunoactivity. Extracts, equivalent to 1000 cells, were analyzed for telomerase activity with telomeric repeat amplification protocol (TRAP) (Kim *et al.*, 1994; Weinrich *et al.,* 1997).

Clonal Culture of Sorted E-NCAM−/A2B5− E14.5 Cells

E14.5 neural tube cells were freshly dissected and dissociated by using 0.05% Trypsin–EDTA. Suspended cells were stained with E-NCAM and A2B5 antibody for 1 h on ice. After cells were washed three times with culture medium, they were stained by FITC-conjugated secondary antibody for 30 min on ice. Single cells were filtered through a 70-μm cell strainer and sorted by the antigen expression on a FACS cytometer. Both negative and positive populations (Lin− and Lin+) were collected and plated at a density of 50–100 cells per 35-mm dish coated with FN with NEP-basal medium and 10% CEE. Cells were grown for 8 days and further split at a density of 1 cell per well into a 96-well plate coated with PLL/LAM. These single cells were cultured with differentiating medium that lacked CEE, but contained bFGF (20 ng/ml), platelet-derived growth factor BB (PDGFBB, 10 ng/ml; Upstate), retinoic acid (17.5 ng/ml; Sigma), Neurotrophin-3 (NT-3, 10 ng/ml; Peprotech), and triiodothyronine (T3, 30 ng/ml; Sigma). After being cultured in differentiating medium for another 16 days, cells were analyzed by triple-labeling immunocytochemistry.

RESULTS

Neuroepithelial Cell Ultrastructural Features

In order to study the properties of NEP stem cells, we examined E10.5 and E14.5 neural tubes. E10.5 neural tubes contain primarily NEP cells (Kalyani *et al.,* 1997), while E14.5 neural tubes contain postmitotic neurons, neuronal

TABLE 2
Summary of Markers Whose Expression Was Not Detected in NEP Cells

Markers	NEP	Expression
EGFR	-	Later appearing NSCs/Differentiated cells
E-NCAM	-	NRP/Neurons
A2B5	-	GRP/Oligodendrocyte precursors
PLP/DM20	-	GRP/Oligodendrocytes
Nkx2.2	-	GRP/Oligodendrocytes
GalC	-	Oligodendrocytes
O4	-	Oligodendrocytes
βIII tubulin	-	Neurons/Neuronal precursors
MAP2	-	Neurons/Neuronal precursors
NF	-	Neurons
PDGFRα	-	Astrocytes/Oligodendrocytes/Neurons
RC1	-	Astrocytes/Radial glia cells
GFAP	-	Astrocytes/Radial glia cells
S-100β	-	Astrocytes/Ependymal cells
CD44	-	Astrocytes/Injured neurons

Note. The column on the right lists the cells that express these markers.

precursors, as well as glial precursor cells and a small amount of multipotent NEP cells. Sections from cranial and caudal regions were processed for light microscopy, TEM, and low-vacuum SEM (Fig. 1). At both E10.5 and E14.5, the ventricular surface of the neuroepithelial tissue appeared smooth. Cilia were detected, but no single long cilium was observed at either stage of development (Figs. 1b, 1e, and 1g–1i). Cells in the ventricular zone did not appear morphologically unique and appeared similar at both stages examined (compare Figs. 1a and 1d). Cells at E10.5 spanned the entire dimension of the tube from the luminal surface to the external lamina, while most cells in the ventricular zone at E14.5 spanned less than one-third of the dimension of the neural tube (Figs. 1a and 1d). Ventricular zone cells appeared barely differentiated and lacked any obvious ultrastructural features. Cytoplasm contained smooth and rough endoplasmic reticulum, and occasional nuclei undergoing division were observed. Cells were tightly packed, and junctions (gap or tight) were seen at the luminal surface of the cells (Figs. 1c and 1f) as well as in deeper layers. Junctions were also seen between ventricular zone cells at E14.5.

In order to verify that NEP cells do have gap junctions, we performed RT-PCR analysis to detect connexins, a component of gap junctions (reviewed in Rozental *et al.*, 2000). PCR amplification results suggest that at least connexin43 (Cx43) and connexin45 (Cx45) (but not Cx26) were present (Fig. 1j) in both stages. Immunocytochemistry with an antibody specific to Cx43 confirmed its expression at E10.5 (Fig. 1k). Both Cx43 and Cx45 levels were significantly lower at E14.5 (Fig. 1j), and levels of Cx43 were almost undetectable by immunocytochemistry (Fig. 1l). Thus, at least some of the junctions seen by EM are gap junctions, and the specific composition changes developmentally. Overall, the results suggest that ventricular zone cells are similar at E10.5 and E14.5 and do not appear to be morphologically distinct from more differentiated cells present outside the ventricular zone.

NEP Cells Do Not Express Early Differentiation Markers

We have previously shown that NEP cells isolated from E10.5 rat neural tubes are multipotent NSCs that are capable of differentiating into neurons, astrocytes, and oligodendrocytes (Kalyani *et al.*, 1997, 1998). To determine whether NEP cells can be distinguished from other cells in the CNS, we examined the expression of markers characteristic of early differentiating neurons, astrocytes, and oligodendrocytes by RT-PCR and immunocytochemistry. Levels were normalized by concurrently examining the expression of the housekeeping gene glyceraldehyde-3-phosphate dehydrogenase (G3PDH) (Fig. 2a). EGFR, PDGFRα, neurofilament (NF), proteolipid protein PLP (PLP/DM20), glial fibrillary acidic protein (GFAP), A2B5, and E-NCAM, which have been shown to be expressed by early precursor cells or differentiated cells, were examined (reviewed in Gage, 2000; Rao, 1999; Garcia-Verdugo *et al.*, 1998). NEP cells do not express EGFR (Fig. 2a), a receptor that is expressed by later appearing NSCs (Reynolds *et al.*, 1992; Tropepe *et al.*, 1999) and by multiple cell types later in development (Lazar and Blum, 1992). NEP cells do not express PDGFRα (Fig. 2a), a receptor that is an early marker for oligodendrocyte precursors (Pringle *et al.*, 1992, 1998; Pringle and Richardson, 1993; Ellison and De Vellis, 1994) and is expressed by neuronal precursors from the cortex as well (Williams *et al.*, 1997; Andrae *et al.*, 2001). NEP cells do not express any neuronal marker we tested, such as E-NCAM (Fig. 2b), NF (Fig. 2a), β-III tubulin, or MAP-2 (data not shown). In addition, oligodendrocyte markers such as PLP/DM20, which is expressed early in development (LeVine *et al.*, 1990), A2B5, GalC, and O4 antigens were not detected (Figs. 2a and 2d; and data not shown), though we could readily detect their expression either by PCR (PLP/DM20) or by immunocytochemistry at later stages in development. We also failed to detect the expression of astrocytic markers GFAP (Fig. 2a), RC1, S-100β, and CD44 (data not shown) (Adami *et al.*, 2001; Edwards *et al.*, 1990; Moretto *et al.*, 1993). Thus, our results indicate that NEP cells present in the ventricular zone of E10.5 rats can be distinguished from other cells present in the CNS by the absence of early neuronal and glial markers, such as EGFR, PDGFRα, E-NCAM, A2B5, and in particular GFAP and S-100β. Absence of these markers in most cells within the proliferating ventricular zone was confirmed by immunocytochemistry at E14.5 and later stages (E16–P1; data not shown).

The absence of neuronal, astrocytic, and oligodendroglial markers in cells that are capable of generating neurons, astrocytes, and oligodendrocytes in culture was the criteria used to define a NEP stem cell population for subsequent analysis. A summary of the tested markers that are not expressed by NEP cells is listed in Table 2.

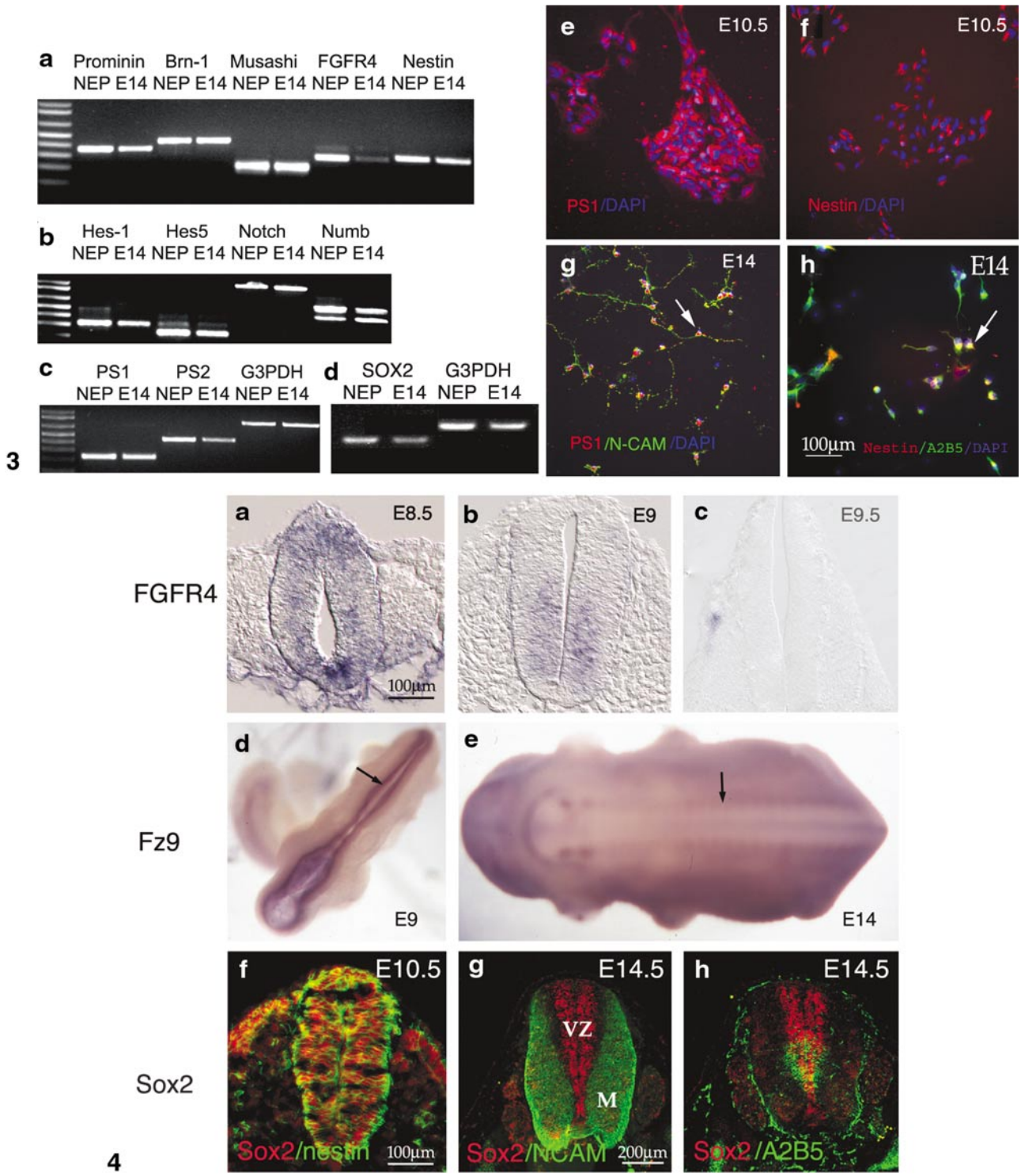

FIG. 3. Comparison of expression pattern of selected genes in NEP cells and E14.5 neural tube. Neural tubes were dissected at E10.5 and E14.5 and processed for RT-PCR by using a battery of primers (a–d). Acutely dissociated cells were fixed and processed for immunocytochemistry to detect expression of PS1 or Nestin (e–h). Primers used were tested for specificity, and samples were run in duplicate. Levels of expression were estimated by normalizing levels with the expression of G3PDH. Experiments were repeated with independent isolations of samples at least three times. Prominin, Brn1, Musashi, Nestin, Hes1, Hes5, Notch, Numb, PS1, and PS2 are expressed at equivalent levels at E10.5 or E14.5 (a–d). Sox2 and FGFR4 expression was dramatically reduced at E14.5. Expression of PS1 and Nestin was detected in

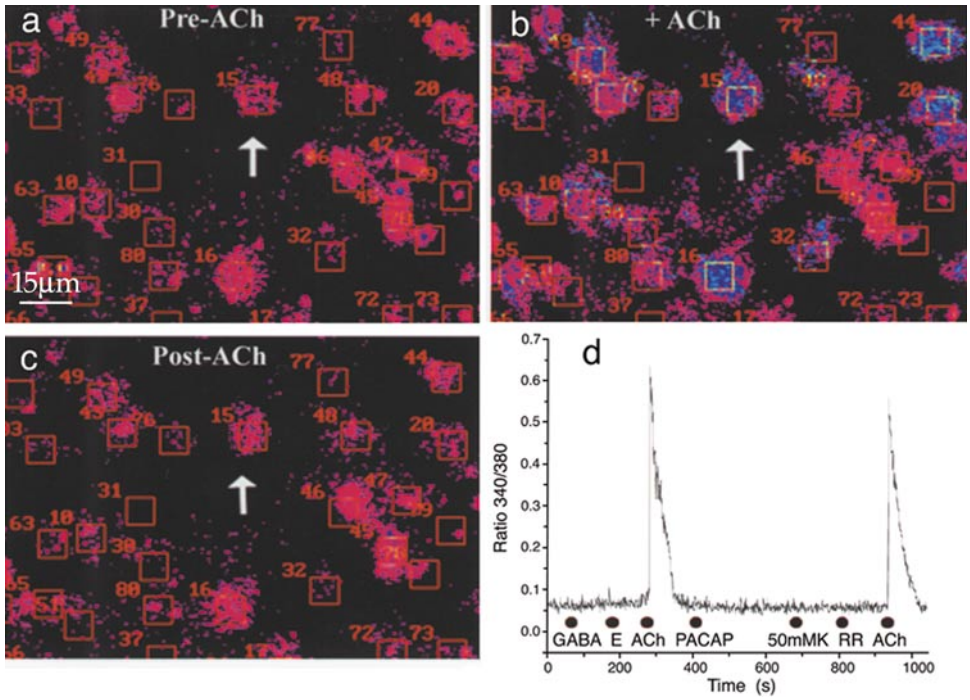

FIG. 5. Rat embryonic NEP cells from E10.5 have a limited neurotransmitter receptor response. E10.5 NEP cells were dissected and maintained in culture for 2 days and their response to neurotransmitter application assessed by Fura imaging (see Materials and Methods). (a) Pseudocolored ratiometric image of a representative field of acutely cultured cells loaded with the Ca^{2+} indicator dye fura 2 shows low resting intracellular Ca^{2+} levels (pink). Regions of interest (ROIs, red boxes) were drawn over each cell and the ratio of fluorescence at 340 and 390 nm was measured on-line within each ROI. The arrow indicates ROI 15 as the cell for which the entire time series is shown in (d). The image in (a) was taken 20 s before application of 500 μM ACh (Pre-ACh). (b) This ratioed image was captured during the peak of the ACh response (+ ACh). The pseudocolor change from pink to blue to white indicates an approximately 200 nM increase in intracellular Ca^{2+} based on a standard two-point calibration. (c) This ratioed image was captured 2 min after ACh application (Post-ACh) and shows that intracellular Ca^{2+} returned to baseline levels. (d) A recording of intracellular Ca^{2+} levels is presented from a representative cell (ROI 15, arrow in a–c) and shows that the cells responded robustly to repeated applications of 500 μM ACh, but that they did not respond to applications of 500 μM GABA or glutamate (E), 100 nM PACAP, 50 mM K Ringer's, or control Ringer's (RR).

Multiple Markers Present on NEP Cells Are Also Detectable on Restricted Glial and Neuronal Precursor Cells

Early studies show that a number of molecules are expressed in early embryonic stages and have great importance in embryonic neural development. These include Prominin1 (Weigmann *et al.*, 1997), Musashi (Kaneko *et al.*, 2000), transcription factors containing POU domains such as Brain1 (Brn1) (Josephson *et al.*, 1998), bHLH domain containing factors such as Numb, NeuroD, downstream effectors of Notch signaling, Hes1, and Hes5 (Kageyama and Ohtsuka, 1999; Zhong *et al.*,

cultured NEP cells (e–f) and E14.5 neural tube cells (g, h). DAPI staining (blue in all figures) was used to detect the presence of all cells. Arrows point to samples of PS1+/E-NCAM+ cells or Nestin+/A2B5+ cells at E14.5.

FIG. 4. FGFR4, Fz9, and Sox2 are downregulated at later stages of development. Mouse embryos were harvested at E8.5, E9.0, E9.5, and E14.0, processed for *in situ* hybridization using probes specific for FGFR4 (a–c) and Fz9 (d, e), and rat embryos were harvested at E10.5 and E14.5 for Sox2 expression (f–h). Strong expression of FGFR4 was observed at stage E8.5 (a), while expression was reduced by E9.0 (b) and was lost by E9.5 (c). Fz9 expression was seen in the whole CNS, including the entire neural tube at E9.0 (d, arrow points to the neural tube). At stage E14.5, no expression of Fz9 was seen (e, arrow points to the neural tube). Sox2 expression was seen in most cells of the neural tube of E10.5 rat, and double labeling with Nestin showed coexpression of Sox2 (red in f) and Nestin (green in f). At E14.5, Sox2 expression was seen mainly in the ventricular zone (marked as VZ in g) (red in g and h), and does not overlap with the E-NCAM expression (green in g, marked as M for mantle in g) and differs from the pattern of A2B5 expressing (green in h).

1997), Presenilins (Yang *et al.*, 2000; Handler *et al.*, 2000), and Sox2 (Kishi *et al.*, 2000).

To determine whether multipotent NEP cells express these markers and whether the expression of these markers is sufficient to distinguish NEP cells from other cells present in the developing CNS, we examined their expression by semiquantitative RT-PCR. Acutely dissociated cells were used for all experiments, and controls demonstrating the absence of E-NCAM, A2B5, EGFR, and PDGFRα were always performed before cells were analyzed. Primers were individually tested for their specificity by using positive and negative controls. RT-PCR analysis showed that mRNA of all these genes was present in acutely dissociated NEP cells (Figs. 3a–3d). Similar results were obtained with multiple isolations of NEP cell populations ($n = 3$). In an effort to determine whether the expression of some of these genes is unique to NEP cells, we compared the expression pattern of the above 14 genes between NEP cells and E14.5 neural tube cells. Semiquantitative RT-PCR was used to compare the expression, and the amount of cDNA was normalized to the housekeeping gene G3PDH. Prominin1, Brn1, Musashi, Nestin, Notch, Numb, Hes1, Hes5, PS1, and PS2, were all detected at E14.5, and levels appeared similar at both stages (Figs. 3a–3c), indicating that these genes were likely expressed by later appearing cells as well. Fz9 (data not shown), FGFR4 (Fig. 3a), and Sox2 (Fig. 3d) were the only genes tested that appeared to be downregulated at E14.5.

To confirm our RT-PCR results, we tested the expression of several of these genes with antibody staining and show the results for two such proteins tested: PS1 and Nestin (Figs. 3e–3h). Staining confirmed the RT-PCR results that both NEP cells and E14.5 neural tube-mixed cells express these markers. Staining sections with Sox2 antibodies showed that expression was limited to the ventricular zone and was largely absent in early born neurons at E14.5, which were labeled by E-NCAM staining (Figs. 4f–4h). Staining in culture suggested that downregulation appeared to coincide with the acquisition of E-NCAM and A2B5 immunoreactivity, but some double-positive cells could be identified (data not shown). *In situ* hybridization analysis of FGFR4 and Fz9 expression confirmed our RT-PCR analysis. At E8.5–E9, mouse neural tubes (equivalent to E10.5 in rats) primarily consist of NEP cells (Mujtaba *et al.*, 1999), and both FGFR4 and Fz9 were detected (Figs. 4a, 4b, and 4d). The expression of FGFR4 is undetectable by E9.5/E10 (Fig. 4c), while the expression of Fz9 in the neural tube is reduced by E9.5/10 (data not shown; see, however, Van Raay *et al.*, 2001) and absent at E14.0 (Fig. 4e). Thus, NEP cells *in vitro* and *in vivo* express FGFR4, Fz9, and Sox2, and levels are rapidly downregulated as cells differentiate. Despite the presence of a morphologically detectable ventricular zone, we could not detect Fz9 or FGFR4 expression by *in situ* hybridization after E12.5, though we could identify Sox2 expression in the ventricular zone until at least E16.

NEP Cells Respond to Acetylcholine but Not to Other Neurotransmitters

Another potential useful method of distinguishing NEP cells from other cells is by analyzing their response to neurotransmitters. It has been suggested that neurotransmitters, in addition to cytokines, may regulate proliferation and differentiation of NSCs and precursor cells (Nguyen *et al.*, 2001). We chose to analyze the effect of glutamate, GABA, ACh, and PACAP. Stimulation by glutamate and GABA has been shown to increase cell proliferation in the ventricular zone while decreasing cell proliferation in the subventricular zone (SVZ) (Haydar *et al.*, 2000). PACAP is abundantly expressed in early development and its receptor is expressed in the ventricular zone at E13.0 (Waschek *et al.*, 2000).

To test whether functional neurotransmitter receptors and their transduction machinery were present on rat NEP cells and to determine their response profile, we used the membrane permeant Ca^{2+} indicator dye Fura-2 AM to visualize changes in intracellular Ca^{2+} concentrations ($[Ca^{2+}]_i$). Figures 5a–5c show a series of pseudocolor ratiometric images of an enlargement of a region from a field of recorded cells before, during, and after application of ACh. In the presence of ACh, $[Ca^{2+}]_i$ increased in about half of the cells. Three coverslips from two different isolations were imaged, and the numbers of cells that responded to 500 μM ACh from the three experiments were 23 of 45 (51%), 5 of 11 (45%), and 17 of 29 (59%). These data indicate that, on average, 52% of the cells in a field of view were capable of responding to ACh. We also tested 500 μM GABA, 500 μM L-glutamate, and 100 nM PACAP. There was no response to any of these neurotransmitters. To determine whether the cells were expressing voltage-gated Ca^{2+} channels, we applied elevated K^+ RR to depolarize the cells. In electrically excitable cells, the K^+-induced depolarization will open voltage-gated Ca^{2+} channels and $[Ca^{2+}]_i$ will increase. We did not see any responses to elevated K^+ or to control applications of RR. As shown in Fig. 5d, a second application of ACh was still capable of eliciting a Ca^{2+} response, indicating that the lack of response to the chemicals following the first ACh application was not due to cell rundown. Our data suggest that NEP cells do not respond to PACAP, glutamate, or GABA, but have a robust response to ACh. Thus, the response profile of NEP cells differs from that reported for human NSCs (Piper *et al.*, 2001), NRP (Kalyani *et al.*, 1998), GRP (David Piper, personal communication), and oligodendrocyte precursor cells (Bergles *et al.*, 2000).

Hoechst 33342 Staining and Rhodamine-123 Levels Do Not Serve to Distinguish NEP Cells from Other Dividing Precursors

In addition to positive and negative selection with cell surface markers, intrinsic properties of stem cells have been utilized to distinguish stem cell populations from mixed cultures of cells. In adult tissue, Hoechst dye and

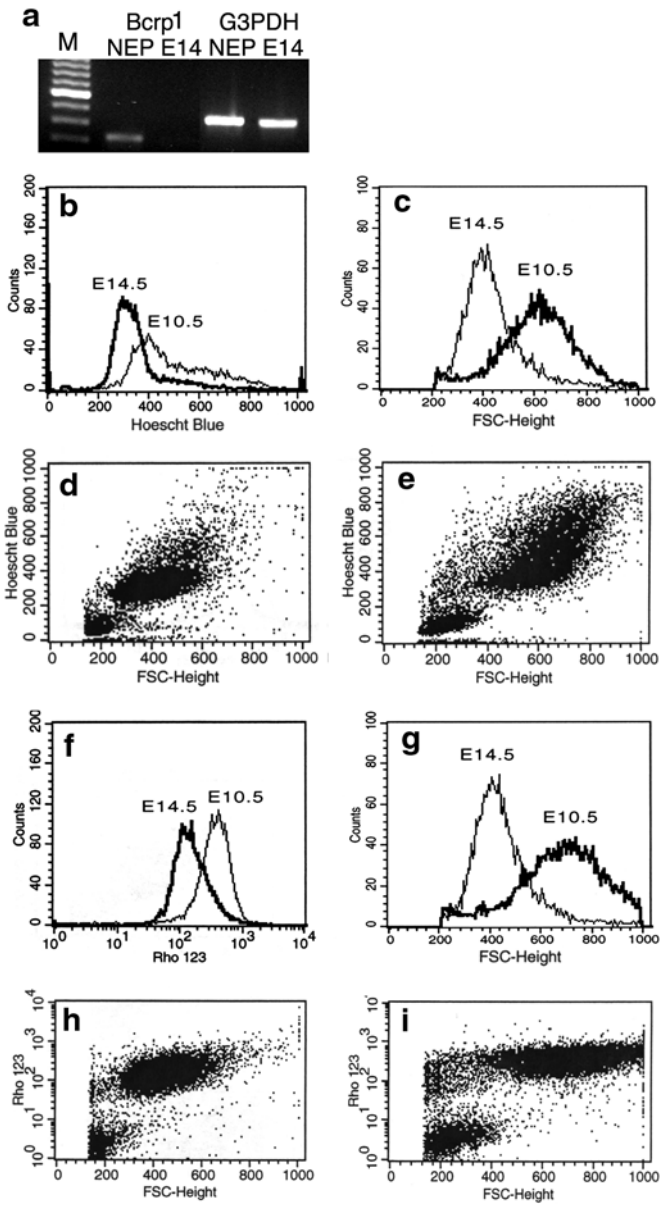

FIG. 6. Flow cytometric cell sorting analysis of Hoechst 33342- and rhodamine-123-stained cells. E10.5 (NEP cells) and E14.5 (mixed cells) neural tubes were dissociated and cells were harvested for RT-PCR (a) or flow cytometric analysis of Hoechst 33342 and rhodamine-123 labeling (b–i). RT-PCR analysis showed that the expression of Bcrp1 transporter is downregulated during development (a). For the Hoechst 33342 and rhodamine-123 analysis, samples were run on the same day under identical conditions. Plots of fluorescence intensity vs FSC-height were prepared and representative results from one such experiment were shown (d–e, h–i). All experiments were performed with at least three different isolations of cells. Comparison of the Hoechst 33342 staining shows that the uptake is virtually similar in the two populations of cells (compare d and e). The small shift to the right is likely due to the somewhat larger size of the E10.5 cells (compare b and c). Similar results were observed when rhodamine-123 was used (h–i). Rhodamine-123 levels were slightly higher in NEP cells than in E14.5 neural tube cells (compare f and g).

rhodhamine-123 labeling have been used to identify quiescent stem cell populations that show the largest self-renewal probability. Low Hoechst 33342 dye fluorescence, low rhodamine-123 uptakes, and forward vs side scatter properties have been used to isolate stem cells from multiple tissues (Leemhuis *et al.*, 1996; Radley *et al.*, 1999).

To test whether similar strategies could be used to distinguish fetal NSCs, we harvested E10.5 NEP cells, which are comprised of a predominantly NSC population and compared their properties with those of a mixed population of neural tube cells isolated from E14.5. Expression of Bcrp1 transporter, reported to be an efficient Hoechst 33342 efflux pump (Scharenberg *et al.*, 2002), is readily detectable in acutely dissociated NEP cells (Fig. 6a). Expression is rapidly downregulated and is absent after 30 cycles of amplification from E14.5 neural tubes cells (Fig. 6a), suggesting Hoechst staining properties may serve to distinguish NSCs from other precursor populations. However, the overall levels of Hoechst fluorescence in NEP cell populations (E10.5) appeared similar to the population of mixed cells (E14.5), where NEP cells constitute less than 10% of the cell population (Fig. 6b). No shoulder of low Hoechst dye staining uptake could be identified in the E10.5 population of multipotent cells, and no peak of low Hoechst-expressing cells could be distinguished in the E14.5 mixed populations of multipotent cells, precursor cells, and differentiated cells. Comparison of the overall profiles of the two cell populations indicated a small shift to the right (high Hoechst) rather than to the left (low Hoechst) in the E10.5 NEP cell population. This shift may be attributed to the larger nuclei in NEP cells, whose size is larger than E14.5 neural tube cells as shown in Fig. 6c. The larger cell size was confirmed visually and by FACS examining the forward vs side scatter properties (data not shown).

Essentially identical results were obtained when rhodamine-123 was used to determine whether a discrete stem cell population could be identified. Figure 6f shows that the level of rhodamine-123 uptake was equivalent in NEP cells when compared with the E14.5 population of mixed cells. As in the case of Hoechst staining, the slight shift of rhodamine-123 curve to the right in NEP cells can be attributed to larger cell size of the multipotent NEP cells relative to the mixed lineage cells (Fig. 6g) and is not statistically significant.

Analysis of the Hoechst blue/red staining pattern did not reveal a side population that in other systems is thought to identify long-term, self-renewing precursors. The small population of cells present near the bottom of the plots (Figs. 6d, 6e, 6h, and 6i) was likely compound of dead cells, and this was confirmed by plating this population in NEP medium and examining the growth of these cells. Cells appeared dead, and no surviving cells could be detected even after prolonged periods in culture (data not shown).

While neither Hoechst 33342 nor rhodamine-123 staining was sufficient to distinguish NEP cells from NRP and GRP cells, we noted that there was a 40-fold difference in

staining intensity for both Hoechst and rhodamine staining in E10.5 and E14.5 cell populations (Figs. 6b and 6f). This raised the possibility that the NEP cells may be enriched in the less-stained population. To test this possibility, we stained dissociated E14.5 cell populations with either Hoechst 33342 or rhodamine-123 and harvested the upper ten percent and the lower ten percent of the stained cells and then examined the percentage of A2B5 and E-NCAM cells in these populations. We reasoned that if NEP cells were enriched in this less stained population, then the number of A2B5/E-NCAM-positive cells would be diminished. Figures 7a′ and 7b′ show, however, that this was not the case. The fraction of cells labeled with E-NCAM and A2B5 was similar in both cell populations ($n = 3$). Thus, our data suggest that neither Hoechst dye staining nor rhodamine-123 fluorescence can be used in isolation to purify a NEP stem cell population from E-NCAM and A2B5 immunoreactive precursor cells.

Rhodamine-123 Levels Identify a Slow Dividing Population in Neural Cultures

Fetal NSCs in the developing CNS are rapidly dividing cells, and the rate of cell division is significantly increased during normal development (Takahashi *et al.*, 1999). In other systems, like hematopoietic tissue, where rhodamine-123 staining has been used to detect stem cells, rhodamine-123-negative cells were shown to be slowly dividing cells with extensive self-renewal potential. We therefore tested whether rhodamine-123 could be used to separate slow dividing multipotent NSCs from rapidly dividing precursor cells.

We selected E10.5 and E14.5 cells on the basis of rhodamine-123 fluorescence and cultured the top and bottom 10% of the population in separate 35-mm culture dishes. Cells were pulsed with Brdu for a period of 6 h (approximately one cell cycle duration) prior to fixing, and the number of cells incorporating Brdu was assessed by immunocytochemistry. Cells in both fractions appeared healthy and survived well. However, as seen in Fig. 7, the percentage of dividing cells was about 12% (average when counted in 10 fields) in the Rho-high cells, and there was almost no Brdu incorporation in the Rho-low cells. (Results are presented from E14.5 isolations, but identical results were obtained with cells isolated from E10.5 embryos.) Thus, a clear-cut difference in cell division was observed. Cells with low rhodamine uptake divided less frequently than cells with high rhodamine uptake. Similar results were seen with Hoechst dye selection (data not shown). Slow dividing cells (Rho-low), however, were not identical in the two populations. At E14.5, slowly dividing cells included E-NCAM+ and A2B5+ immunoreactive cells (Fig. 7). Thus, in the case of fetal neural cells, rhodamine-123 efflux can be used to distinguish actively dividing cells from slower dividing cell population, and the high uptake of rhodamine-123 is correlated with cell proliferation.

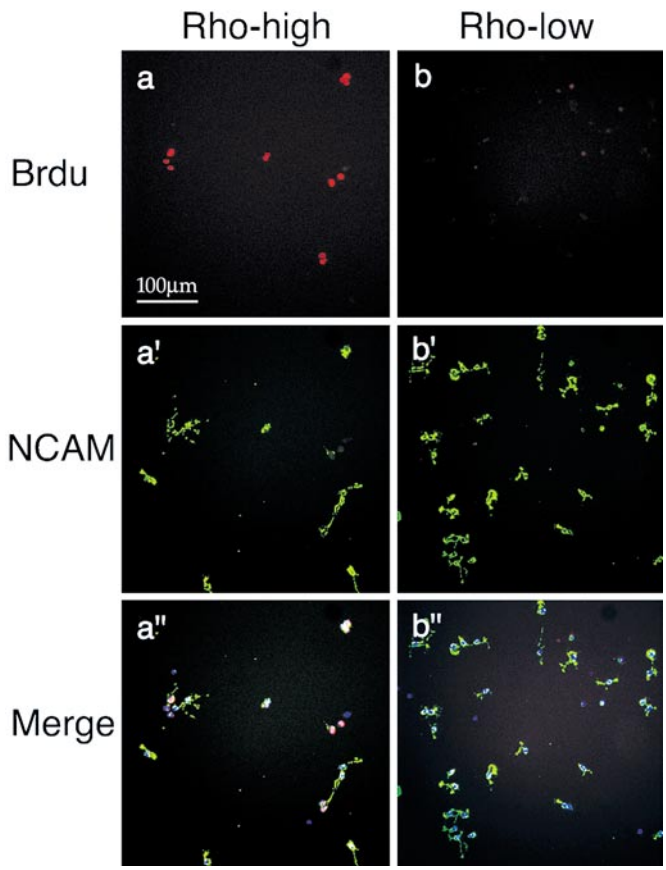

FIG. 7. Rhodamine-123 staining can distinguish rapidly dividing cells from slowly dividing cells. E14.5 (mixed cells) neural tubes were dissociated, and cells were harvested and processed for flow cytometric analysis of rhodamine-123 levels. Two populations were collected. The top (Rho-high) and the bottom (Rho-low) 10% of the population were collected. After plating for 1 day for the recovery from sorting, both populations of cells were pulsed with Brdu for 6 h (approximately one cell cycle; Takahashi *et al.*, 1995; our unpublished results). Cells were fixed immediately after the pulse and processed for Brdu incorporation and E-NCAM expression. (a) Around 12% of the Rho-high uptake cells are dividing (a, quantified in 10 fields), while none of the Rho-low uptake cells are Brdu-positive (b). E-NCAM staining of the same fields as in (a) and (b) were shown in (a′) and (b′). The merge graphs with DAPI staining were shown in (a″) and (b″). Note that E-NCAM cells did not segregate to either the Rho-high or the Rho-low populations.

NEP Cells Have Measurable Telomerase Activity

A hallmark of most stem cells is the presence of telomerase activity (reviewed in Meeker and Coffey, 1997). In the CNS, Tert expression is rapidly downregulated (Fig. 8a) and little activity is detected after E15.5 or in postmitotic neurons (Fig. 8b; Klapper *et al.*, 2001; Kruk *et al.*, 1996). These data raised the possibility that Tert expression and its activity could not be used to identify stem cells. To test this possibility, we compared the telomerase activity of

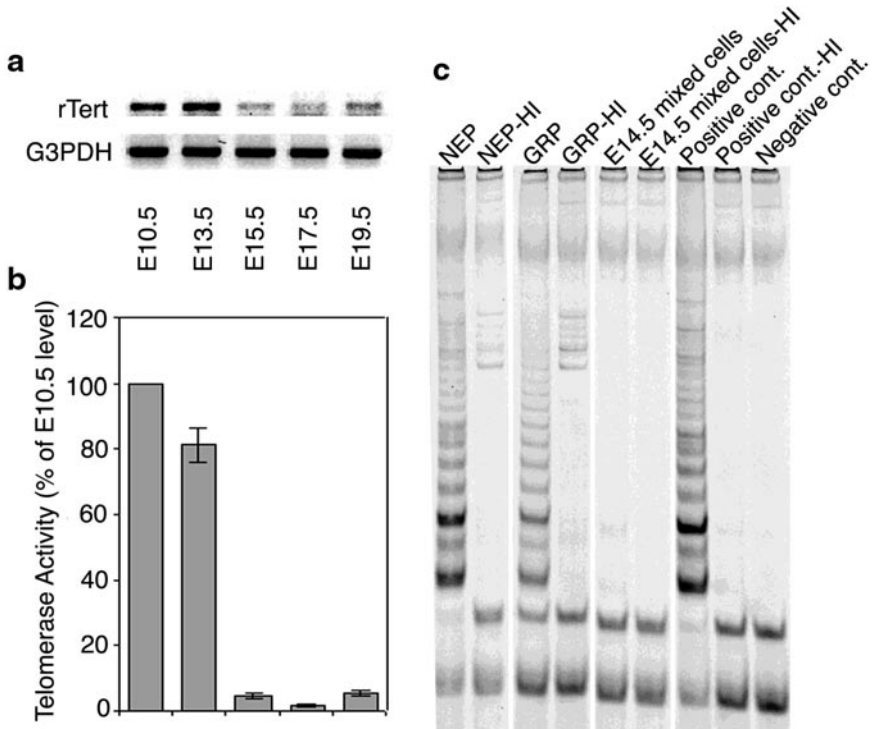

FIG. 8. NEP cells have detectable telomerase activity. Telomerase activity and Tert levels were examined in acutely dissociated NEP cells, E14.5 cells, or GRP cells isolated by selecting for A2B5+ cells using FACS either by RT-PCR (a) or a TRAP assay (b and c). RT-PCR analysis of neural tubes from five rat stages showed that Tert levels dropped dramatically after E15.5 (a). PCR amplification products were obtained with the primers listed in Materials and Methods. The activity of telomerase decreased remarkably during development (b). Little activity can be detected after E15.5. Extracts equivalent to 1000 cells were analyzed for telomerase activity with standard TRAP assay. Both NEP cells and GRP cells have detectable telomerase activity, while the level in NEP cells is higher than that in GRP cells. E14.5 neural tube mixed cells has barely detectable telomerase activity (c). HI samples are heat-inactivated controls.

E10.5 multipotent NEP cells, E14.5 cells with neuronal and glial precursors present together, as well as a purified glial precursor population (GRP) selected on the basis of A2B5 immunoreactivity (Rao *et al.*, 1998). Samples were run in parallel, and comparisons were made from assays done simultaneously (see Materials and Methods). We noted high levels of telomerase activity in NEP cells (Figs. 8b and 8c). Levels in NEP cells were comparable to levels seen in immortalized or transformed cells, such as PC12 cells (unpublished results). Telomerase activity was lower in A2B5-positive GRP cells but was nevertheless readily detectable (Fig. 8c). Telomerase activity was barely detectable in mixed populations of cells isolated from E14.5 neural tubes, which contain postmitotic neurons, neuronal precursors, as well as multipotent NEP cells and glial precursors. This suggests that levels are rapidly downregulated as cells differentiate toward the neuronal lineage as has been previously reported (Kruk *et al.*, 1996) and the number of NSCs has rapidly declined. Thus, NEP cells, consistent with their NSC characteristics, express high levels of telomerase activity. Telomerase activity, however, does not serve to distinguish NSCs from more restricted precursor cells, such as glial precursors.

Multipotent Stem Cells Can Be Isolated from E14.5 Neural Tube Cells by the Absence of E-NCAM and A2B5 Expression

Our results suggest that negative selection using cell surface markers can be used to enrich multipotent stem cells as has been described in other systems (Rasmussen *et al.*, 2002). To test this, we isolated E-NCAM−/A2B5− cells from E14.5 neural tube mixed cells by FACS and examined their differentiation potential in clonal density and high density cultures.

The lowest 10% of the E-NCAM−/A2B5− fraction (Fig. 9b) were sorted by FACS selection, and the purity of the population was confirmed by immunostaining with either E-NCAM or A2B5 1 day after FACS (Figs. 9d and 9e). More than 95% of the cells were E-NCAM−/A2B5− cells (Fig. 9c). A large proportion of the cells divided in culture as assessed by Brdu incorporation after a 3-h pulse (Fig. 9f). When E-NCAM−/A2B5− cells were plated on PLL/LAM-

coated dishes at high density, these cells were able to differentiate into the major cell types present in the CNS as assessed by GalC, β-III tubulin, and GFAP immunoreactivity (Figs. 9g–9i).

To test the ability of individual cells to differentiate, we plated E-NCAM−/A2B5− cells at low density (50–100 cells/dish) on FN-coated dishes. Cells divided rapidly and formed colonies as previously described (Kalyani *et al.*, 1997) for NEP cells. Colonies had a uniform morphology and grew as compact, tightly packed groups of cells (Fig. 9j). The morphology of these colonies is distinct from the colonies generated from E-NCAM+/A2B5+ cells (Figs. 9k–9m) that were plated at the same time as a control. E-NCAM−/A2B5− colonies were allowed to grow for a period of 8 days, and the medium was replaced to promote differentiation. Cells were cultured in differentiating medium for an additional 16 days and then processed for immunocytochemistry. Two examples of multipotent colonies were shown (Figs. 9n and 9o). The number of multipotent colonies was assessed by examining two sets of clonal cultures. As described with E10.5 rat (Kalyani *et al.*, 1997) and E8.5 mouse stem cell cultures (Mujtaba *et al.*, 1999), no unipotent colony was detected. All colonies contained at least two phenotypes: GFAP+/βIII tubulin+ (data not shown). In addition, 20% of the colonies ($N = 2$) contained all three phenotypes. In contrast, no multipotent colony was detected in the E-NCAM+/A2B5+ clones (data not shown). Thus, our results suggest that multipotent stem cells can be distinguished from a mixed population by the absence of E-NCAM and A2B5 immunoreactivity.

DISCUSSION

It has been difficult to determine what properties are characteristic of NSCs because it has been difficult to obtain pure populations of these cells for analysis. Neurosphere cultures contain a small fraction of NSCs, while the adult ependymal and subventricular zones contain mixed populations of cells. We have taken advantage of our observation that the NEP cells in the proliferating neural tubes (along the entire rostrocaudal axis) at early embryonic ages are predominantly multipotent NSCs and share similar self-renewal and differentiation properties. We have harvested these cells and obtained an overall profile of the properties that characterize fetal NSCs. Our results suggest that the fetal NSCs (NEP cells) present in the embryonic ventricular zone lack obvious cilia, possess gap junctions, and appear ultrastructurally indistinguishable from other early immature cells. NSCs can be distinguished from other cells in the CNS primarily by the absence of specific markers. Telomerase activity, and Bcrp1, Sox2, FGFR4, and Fz9 expression appear to be present in fetal NSCs, but no single marker alone can be used to identify NSCs. Strategies that have been used to select NSC populations from adult tissues, such as rhodamine-123 labeling, Hoechst dye efflux, and telomerase levels, can be used to detect the presence of dividing precursor cells in a mixed population but cannot be used to distinguish between stem and precursor cells.

Our results suggest that antibodies to EGFR, PDGFRα, A2B5, E-NCAM, and GFAP may be used to deplete more differentiated cells and thereby enrich for NSCs. EGFR, which is expressed on neurons (Misumi and Kawano, 1998), astrocytes (Nieto-Sampedro *et al.*, 1988), oligodendrocytes, and oligodendrocyte precursors, but not on ventricular zone cells in early development, may be particularly useful as an early selection marker. EGFR has been shown to be expressed by adult multipotent NSCs as well (Okano *et al.*, 1996) and may therefore serve to distinguish between these populations of stem cells at stages of development when both fetal and adult type NSCs are present (E14.0 to adult). Absence of PDGFRα expression may be useful in distinguishing multipotent cells from oligodendrocyte precursors. Polyclonal antibodies to PDGFRα have been used successfully to positively select oligodendrocyte precursors and could be used to deplete these cells from mixed populations as well (Pringle *et al.*, 1992). A2B5 and E-NCAM expression has been demonstrated on more restricted precursor cells as well as on their differentiated progeny. The epitopes recognized by these antibodies are absent, however, from NEP stem cells (Kalyani *et al.*, 1997, 1998) and most adult NSC populations (see however Marmur *et al.*, 1998). These antibodies could reliably distinguish between NEP cells and other dividing precursor cell populations (NRP and GRP cells).

Distinguishing NSCs from GFAP-expressing cells is of importance as at least some GFAP-expressing cells undergo self-renewal and have the capability of differentiating into neurons, astrocytes, and oligodendrocytes (Laywell *et al.*, 2000; Johansson *et al.*, 1999). Early developing ventricular zone NSCs and most neonatal SVZ precursor cells do not express GFAP, suggesting that at most, some NSCs express GFAP (see for example Chiasson *et al.*, 1999). Our results suggest that RC1 and CD44 may be likely candidates for separating multipotent NSCs from astrocytes and radial glial cells (Alfei *et al.*, 1999; Blass-Kampmann *et al.*, 1997). We have used such a depletion strategy using multiple cell type-specific markers successfully in enriching NSCs populations from human fetal tissue cultures (Mayer-Proschel *et al.*, 2002; and Dr. Margot Mayer-Proschel, University of Rochester, personal communication).

Our results suggest that caution must be exercised in using some of the markers that have been thought to define NSCs. Many of the markers that were expressed by multipotent NSCs were also expressed by more restricted precursors or differentiated cells. In particular, Nestin expression has been used routinely to identify NSC populations (Zimmerman *et al.*, 1994). Our present results and those of others show that Nestin expression is seen in restricted precursors (see Results; Rao *et al.*, 1998; Mayer-Proschel *et al.*, 1997), astrocytes (Duggal *et al.*, 1997), radial glia (Takano and Becker, 1997; Li and Chopp, 1999), ependymal cells (Namiki and Tator, 1999), and essentially all dividing

cell populations. Likewise Presenilin, Notch, Numb, Prominin, and other markers need to be coupled with a test of the differentiation potential of the cells to define multipotent stem cells.

Of all the markers examined, three candidate molecules appeared to be relatively specific for fetal stem cells: FGFR4, Fz9, and Sox2. FGFR4 expression has been demonstrated to be restricted to the habenula in adults (Itoh *et al.*, 1994) and its expression has been described in the ventricular zone in rodents (Kalyani *et al.*, 1999), zebrafish (Thisse *et al.*, 1995), and chicken (Marcelle *et al.*, 1994). Fz9 is a member of the *frizzled* gene family (Wang *et al.*, 1999) that is transiently expressed in the ventricular zone and on dissociated NEP cells and is downregulated *in vitro* and *in vivo* after E13.0 (see Results; and Van Raay *et al.*, 2001). Sox2 has been shown to be restricted to the neuroepithelium and to the ventricular zone at later developmental stages (D'Amour and Gage, abstract of 2002 Keystone Symposia; Dr. Larysa Pevny, personal communication). Our results confirm the expression of these three markers in NEP cells/ventricular zone and their reduction or absence in cells that have differentiated at E14.5. Nevertheless it is important to emphasize that no single marker can serve as a universal NSC marker. Sox2 expression for example persists in Nkx2.2 immunoreactive glial precursors (data not shown). Likewise, it is important to note that, so far, we have been unable to detect FGFR4 expression by *in situ* hybridization in the adult SVZ (where multipotent stem cells exist), suggesting that FGFR4 may not be a universal NSC marker. Furthermore, we have been unable to generate antibodies to the extracellular epitopes of Fz9 or FGFR4 to directly test whether a positive selection strategy would work. Nevertheless, these molecules represent likely candidates for a combinatorial positive selection strategy of some NSCs.

Our results analyzing the neurotransmitter response of NEP cells suggest that early NSCs do not respond to most neurotransmitters tested. Acutely dissociated and short passage cultures gave us similar results. The only neurotransmitter that elicited a response is ACh. Roughly half of the NEP stem cells tested (see Results) showed a robust response. The response to ACh is consistent with results on receptor expression (Levey, 1993) and previous results on the effects of ACh and ChAT knockouts on early embryonic development (Gomeza *et al.*, 1999). Our failure to observe any effect of glutamate or GABA application is different from the results observed by Haydar *et al.* (2000). These investigators observed robust effects on proliferation and survival in response to glutamate and GABA application in slice cultures. The absence of mature neurons or neuronal precursors in our cultures may account for the absence of such responses, and further studies will be necessary to verify this observation. We note, however, that we and others have shown early glutamate and GABA responses in neuronal precursors that are present in culture (Kalyani *et al.*, 1998; David Piper, personal communication) of nonpurified or nonselected cells. These results demonstrate an additional difference between early multipotent NSCs and intermediate or more restricted neuronal and glial precursors. Both precursors respond to glutamate application and express AMPA receptors early in development (Pende *et al.*, 1994; Sanchez-Gomez and Matute, 1999; Maric *et al.*, 2000).

Our analysis of rhodamine-123 and Hoechst 33342 efflux suggests that, in early development, no side population of quiescent stem cells with a large self-renewing potential is present. These results are consistent with our early Brdu incorporation studies showing that virtually all cells have divided in culture in a 24-h period (Kalyani *et al.*, 1997) and with a recent report on the properties of adult neural stem cells (Rietze *et al.*, 2001). These results are in contrast with results from adult stem cell cultures, where a side population of quiescent cells has been identified in multiple tissues, including the CNS (Hulspas and Quesenberry, 2000). Our results suggest that, in the fetal stage, the expression of Bcrp1 is not related with the Hoechst 33342 efflux activity. Either the transporter is not activated at early stages or other transporters may exist to aid in the efflux of the Hoechst dye. We interpret these results to suggest that, initially, rapidly dividing stem cells present in fetal development may transit to a quiescent state after the initial phase of repair and regeneration and that these

FIG. 9. FACS sorted E-NCAM−/A2B5− cells form multipotent colonies in culture. E14.5 dissociated neural tube cells were sorted by negative selection (absence of E-NCAM and A2B5) and grown at clonal density (50–100 cells per dish) or high density (10,000 cells/dish) in NEP-basal medium with 10% CEE. As a control, NCAM+/A2B5+ cells were plated at clonal density as well. After 8 days in culture, CEE was withdrawn from the medium and cells were grown further for 5 days before being triple labeled for GalC, βIII tubulin, and GFAP expression. Control cells, which were incubated only with FITC-conjugated secondary antibody, determined the background fluorescence (a). M1 was set according to the control to isolate the bottom 10% of the E-NCAM−/A2B5− population (b). The purity of the collected negative population was checked and was approximately 97% (c). One day after FACS, E-NCAM−/A2B5− cells (Lin−) were labeled with E-NCAM (red in d), A2B5 (red in e), and Brdu (green in f). Dapi counterstaining was used to analyze all cells (d–f). E-NCAM−/A2B5− cells plated at high density were able to differentiate into GalC-, GFAP-, and βIII tubulin-positive cells when they were replated on PLL/LAM-coated dishes for 5 days (g–i). The morphology of E-NCAM−/A2B5− clones (Lin−, j) is uniform and quite different from that of E-NCAM+/A2B5+ cells (Lin+, k–m). Phase pictures were taken 8 days after FACS. Two examples of clones of single E-NCAM−/A2B5− cells that generated GFAP (blue), GalC (green), and βIII tubulin (red) immunoreactive cells were shown (n–o). The scale bar for (d–f) and (n, o) is 50 μm, and the scale bar for (g–m) is 100 μm.

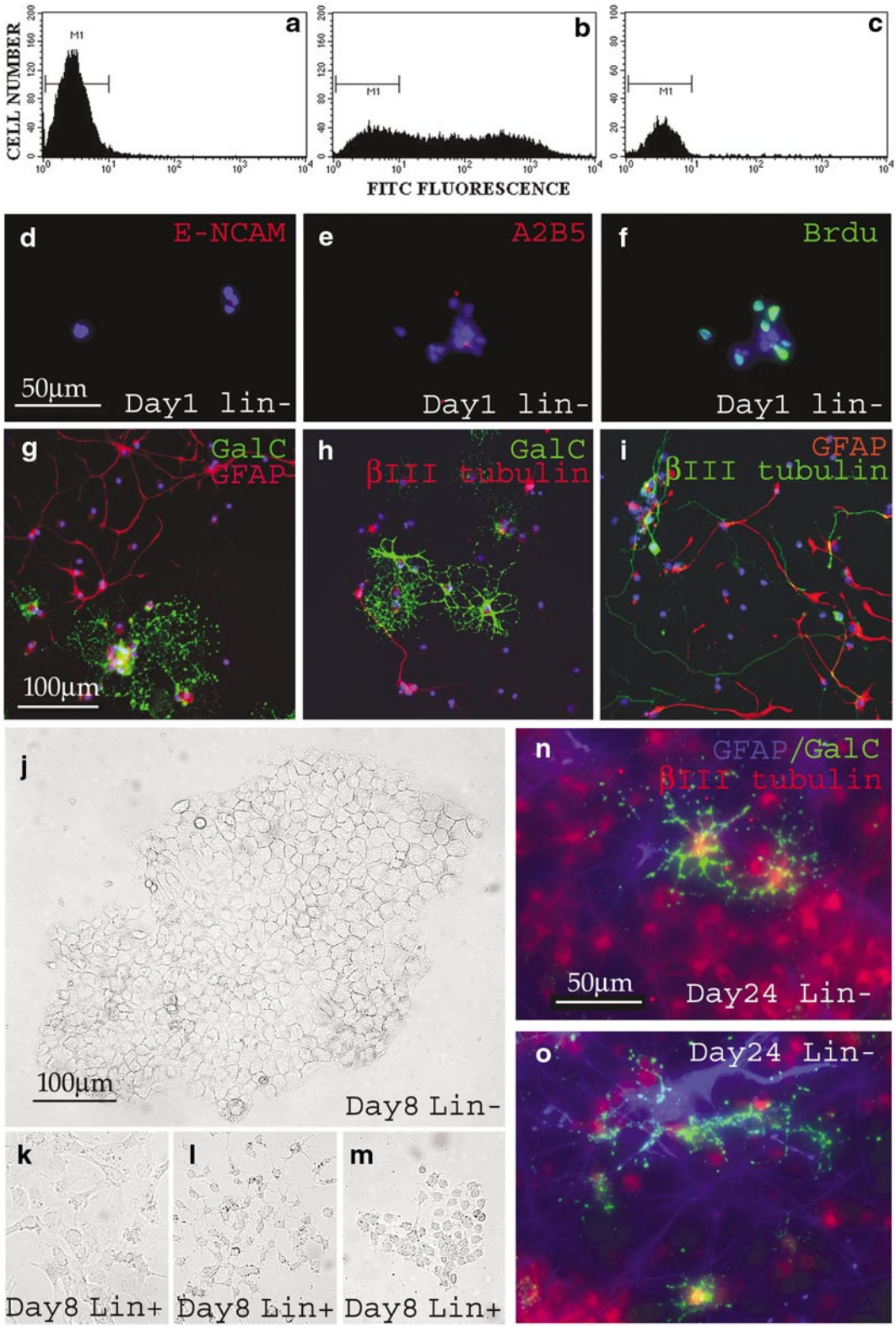

quiescent stem cells may be reactivated during repair and regeneration and no quiescent population has been set aside at this early stage of development.

While we could not use rhodamine-123 or Hoechst 33342 efflux to distinguish between multipotent and more restricted precursors, we could clearly demonstrate a 40-fold difference in cell division in cell populations identified as being homogenous by marker expression. Slow dividing populations present in NEP cell culture, E-NCAM+, or A2B5+ cultures may have special properties that we were unable to discern in a short-term clonal assay. Long-term transplant experiments to compare the fate of these slowly and rapidly dividing populations need to be performed.

Our results analyzing telomerase levels in NSC populations revealed high levels of telomerase in NSC cultures. Our results, however, raise doubts about the utility of using telomerase as a marker of NSCs. We note that high telomerase expression is not unique to NEP cells but that more restricted precursor cells, such as GRP cells, also express high levels of telomerase. Telomerase levels were also high in Rho-high cells (data not shown), suggesting that telomerase expression cannot be used to distinguish between quiescent and rapidly dividing NSCs. More recently, Svendsen and colleagues have suggested that human NSCs may only have low levels of telomerase (Ostenfeld *et al.*, 2000). Analysis of mTert$^{-/-}$ mice, whose fertility progressively decreases, has suggested that, even in later generations of mice that have neural tube defects, the proliferation of ventricular zone NSCs appears normal (Herrera *et al.*, 1999). Finally, Tert expression appears to persist well after its activity cannot be detected, suggesting that immunocytochemistry with anti-Tert antibodies cannot be used to localize NSCs. We conclude therefore that telomerase activity correlates with the NSC state, but its expression or absence cannot be used to identify a population of multipotent NSCs.

In summary, our results suggest that multipotent NEP stem cells can be distinguished from other cells present in the CNS using a combination of positive and negative selection strategies. However, care needs to be taken in selecting appropriate markers. Many markers thought to be unique to multipotent NSCs are present on other precursor cell populations, and generalized strategies of identifying NSCs that have worked well in the adult (telomerase expression, dye efflux, etc.) may not be useful in isolating NSCs during development. Our results, however, provide a series of markers that can reliably distinguish a fetal multipotent NSC population from other neural cells. Future experiments will extend the analysis to NSC populations isolated in different laboratories and at different stages in development.

ACKNOWLEDGMENTS

We thank Drs. Mattson and Cheng for their comments on this manuscript. We gratefully acknowledge the input of all members of our laboratory provided through discussions and constructive criticisms. M.S.R. was supported by the NIA, an NIH FIRST award, an MDA award, and a March of Dimes research grant. We thank Ms. Nancy B. Chandler at the Health Sciences Center's Research Microscopy Facility for expert assistance with the morphological analyses, Dr. Tracy Wright at the Department of Human Genetics, and Mr. Terry Van Raay at the Department of Neurobiology and Anatomy for assistance with the *in situ* hybridization. We thank Mr. Francis J. Chrest in NIA for assistance with FAC sorting. Supported in part by NIH S10-RR-10489 (K.H.A.), NIH R01DK57899 (G.J.S. and L.J.P.), and NIDCD R01DC02994 (M.T.L.). We would like to thank the reviewer for his/her detailed and specific suggestions.

REFERENCES

Adami, C., Sorci, G., Blasi E., Agneletti, A. L, Bistoni, F., and Donato, R. (2001). S100β expression in and effects on microglia. *Glia* **33,** 131–142.

Albertine, K., H., Jones, G. P., Starcher, B. C., Bohnsack, J. F., Davis, P. L., Cho, S. C., Carlton, D. P., and Bland, R. D. (1999). Chronic lung injury in preterm lambs. Disordered respiratory tract development. *Am. J. Respir. Crit. Care Med.* **159,** 945–958.

Alfei, L., Aita, M., Caronti, B., De Vita, R., Margotta, V., Medolago, Albani, L., and Valente, A. M. (1999). Hyaluronate receptor CD44 is expressed by astrocytes in the adult chicken and in astrocyte cell precursors in early development of the chick spinal cord. *Eur. J. Histochem.* **43,** 29–38.

Andrae, J., Hansson, I., Afink, G. B., and Nister, M. (2001). Platelet-derived growth factor receptor-alpha in ventricular zone cells and in developing neurons. *Mol. Cell. Neurosci.* **17,** 1001–1013.

Bergles, D. E., Roberts, J. D., Somogyi, P., and Jahr, C. E. (2000). Glutamatergic synapses on oligodendrocyte precursor cells in the hippocampus. *Nature* **405,** 187–191.

Blass-Kampmann, S., Kindler-Rohrborn, A., Deissler, H., D'Urso, D., and Rajewsky, M. F. (1997). In vitro differentiation of neural progenitor cells from prenatal rat brain: Common cell surface glycoprotein on three glial cell subsets. *J. Neurosci. Res.* **48,** 95–111.

Chiasson, B. J., Tropepe, V., Morshead, C. M., and van der Kooy, D. (1999). Adult mammalian forebrain ependymal and subependymal cells demonstrate proliferative potential, but only subependymal cells have neural stem cell characteristics. *J. Neurosci.* **19,** 4462–4471.

D'Amore, K. A., and Gage, F. H. (2002). Comparison of ES cell, fetal and adult neural stem cells defined by Sox2 expression. Keystone Symposia. Poster 133.

Duggal, N., Schmidt-Kastner, R., and Hakim, A. M. (1997). Nestin expression in reactive astrocytes following focal cerebral ischemia in rats. *Brain Res.* **768,** 1–9.

Edwards, M. A., Yamamoto, M., and Caviness, V. S., Jr. (1990). Organization of radial glia and related cells in the developing murine CNS. An analysis based upon a new monoclonal antibody marker. *Neuroscience* **36,** 121–144.

Ellison, J. A., and De Vellis, J. (1994). Platelet-derived growth factor receptor is expressed by cells in the early oligodendrocyte lineage. *J. Neurosci. Res.* **37,** 116–128.

Gage, F. H. (2000). Mammalian neural stem cells. *Science* **287,** 1433–1438.

Garat, C., Kheradmand, F., Albertine, K. H., Folkesson, H. G., and Matthay, M. A. (1996). Soluble and insoluble fibronectin increases alveolar epithelial wound healing in vitro. *Am. J. Physiol.* **271,** L844–L853.

Garcia-Verdugo, J. M., Doetsch, F., Wichterle, H., Lim, D. A., and Alvarez-Buylla, A. (1998). Architecture and cell types of the adult subventricular zone: In search of the stem cells. *J. Neurobiol.* **36,** 234–248.

Gomeza, J., Shannon, H., Kostenis, E., Felder, C., Zhang, L., Brodkin, J., Grinberg, A., Sheng, H., and Wess, J,. (1999). Pronounced pharmacologic deficits in M2 muscarinic acetylcholine receptor knockout mice. *Proc. Natl. Acad. Sci. USA* **96,** 1692–1697.

Goodell, M. A., Brose, K., Paradis, G., Conner, A. S., and Mulligan, R. C. (1996). Isolation and functional properties of murine hematopoietic stem cells that are replicating in vivo. *J. Exp. Med.* **183,** 1797–1806.

Grynkiewicz, G., Poenie, M., and Tsien, R. Y. (1985). A new generation of Ca^{2+} indicators with greatly improved fluorescence properties. *J. Biol. Chem.* **260,** 3440–3450.

Handler, M., Yang, X., and Shen, J. (2000). Presenilin-1 regulates neuronal differentiation during neurogenesis. *Development* **127,** 2593–2606.

Haydar, T. F., Wang, F., Schwartz, M. L., and Rakic, P. (2000). Differential modulation of proliferation in the neocortical ventricular and subventricular zones. *J. Neurosci.* **20,** 5764–5774.

Herrera, E., Samper, E., and Blasco, M. A. (1999). Telomere shortening in mTR−/− embryos is associated with failure to close the neural tube. *EMBO J.* **18,** 1172–1181.

Hulspas, R., and Quesenberry, P. J. (2000). Characterization of neurosphere cell phenotypes by flow cytometry. *Cytometry* **40,** 245–250.

Itoh, N., Yazaki, N., Tagashira, S., Miyake, A., Ozaki, K., Minami, M., Satoh, M., Ohta, M., and Kawasaki, T. (1994). Rat FGF receptor-4 mRNA in the brain is expressed preferentially in the medial habenular nucleus. *Brain Res. Mol. Brain Res.* **21,** 344–348.

Johansson, C. B., Momma, S., Clarke, D. L., Risling, M., Lendahl, U., and Frisen, J. (1999). Identification of a neural stem cell in the adult mammalian central nervous system. *Cell* **96,** 25–34.

Josephson, R., Muller, T., Pickel, J., Okabe, S., Reynolds, K., Turner, P. A., Zimmer, A., and McKay, R. D. (1998). POU transcription factors control expression of CNS stem cell-specific genes. *Development* **125,** 3087–3100.

Kageyama, R., and Ohtsuka, T. (1999). The Notch-Hes pathway in mammalian neural development. *Cell Res.* **9,** 179–188.

Kalyani, A., Hobson, K., and Rao, M. S. (1997). Neuroepithelial stem cells from the embryonic spinal cord: Isolation, characterization, and clonal analysis. *Dev. Biol.* **186,** 202–223.

Kalyani, A. J., Mujtaba, T., and Rao, M. S. (1999). Expression of EGF receptor and FGF receptor isoforms during neuroepithelial stem cell differentiation. *J. Neurobiol.* **38,** 207–224.

Kalyani, A. J., Piper, D., Mujtaba, T., Lucero, M. T., and Rao, M. S. (1998). Spinal cord neuronal precursors generate multiple neuronal phenotypes in culture. *J. Neurosci.* **18,** 7856–7868.

Kaneko, Y., Sakakibara, S., Imai, T., Suzuki, A., Nakamura, Y., Sawamoto, K., Ogawa, Y., Toyama, Y., Miyata, T., and Okano, H. (2000). Musashi1: An evolutionally conserved marker for CNS progenitor cells including neural stem cells. *Dev. Neurosci.* **22,** 139–153.

Kim, N. W., Piatyszek, M. A., Prowse, K. R., Harley, C. B., West, M. D., Ho, P. L., Coviello, G. M., Wright, W. E., Weinrich, S. L., and Shay, J. W. (1994). Specific association of human telomerase activity with immortal cells and cancer. *Science* **266,** 2011–2015.

Kishi, M., Mizuseki, K., Sasai, N., Yamazaki, H., Shiota, K., Nakanishi, S., and Sasai, Y. (2000). Requirement of Sox2-mediated signaling for differentiation of early Xenopus neuroectoderm. *Development* **127,** 791–800.

Klapper, W., Shin, T., and Mattson, M. P. (2001). Differential regulation of telomerase activity and TERT expression during brain development in mice. *J. Neurosci. Res.* **64,** 252–260.

Kruk, P. A., Balajee, A. S., Rao, K. S., and Bohr, V. A. (1996). Telomere reduction and telomerase inactivation during neuronal cell differentiation. *Biochem. Biophys. Res. Commun.* **224,** 487–492.

Laywell, E. D., Rakic, P., Kukekov, V. G., Holland, E. C., and Steindler, D. A. (2000). Identification of a multipotent astrocytic stem cell in the immature and adult mouse brain. *Proc. Natl. Acad. Sci. USA* **97,** 13883–13888.

Lazar, L. M., and Blum, M. (1992). Regional distribution and developmental expression of epidermal growth factor and transforming growth factor-alpha mRNA in mouse brain by a quantitative nuclease protection assay. *J. Neurosci.* **12,** 1688–1697.

Leemhuis, T., Yoder, M. C., Grigsby, S., Aguero, B., Eder, P., and Srour, E. F. (1996). Isolation of primitive human bone marrow hematopoietic progenitor cells using Hoechst 33342 and Rhodamine 123. *Exp. Hematol.* **24,** 1215–1224.

Levey, A. I. (1993). Immunological localization of m1–m5 muscarinic acetylcholine receptors in peripheral tissues and brain. *Life Sci.* **52,** 441–448.

LeVine, S. M., Wong, D., and Macklin, W. B. (1990). Developmental expression of proteolipid protein and DM20 mRNAs and proteins in the rat brain. *Dev. Neurosci.* **12,** 235–250.

Li, Y., and Chopp, M. (1999). Temporal profile of Nestin expression after focal cerebral ischemia in adult rat. *Brain Res.* **838,** 1–10.

Liu, Y., Wu, Y., Lee, J. C., Xue, H., Pevny, L. H., Kaprielian, Z., and Rao, M. S. (2002). Oligodendrocyte and Astrocyte development in rodents: An in situ and immunohistological analysis during embryonic development. *Glia* **40,** 25–43.

Marcelle, C., Eichmann, A., Halevy, O., Breant, C., and Le Douarin, N. M. (1994). Distinct developmental expression of a new avian fibroblast growth factor receptor. *Development* **120,** 683–694.

Maric, D., Liu, Q. Y., Grant, G. M., Andreadis, J. D., Hu, Q., Chang, Y. H., Barker, J. L., Joseph, J., Stenger, D. A., and Ma, W. (2000). Functional ionotropic glutamate receptors emerge during terminal cell division and early neuronal differentiation of rat neuroepithelial cells. *J. Neurosci. Res.* **61,** 652–662.

Marmur, R., Mabie, P. C., Gokhan, S., Song, Q., Kessler, J. A., and Mehler, M. F. (1998). Isolation and developmental characterization of cerebral cortical multipotent progenitors. *Dev. Biol.* **204,** 577–591.

Mayer-Proschel, M., Kalyani, A. J., Mujtaba, T., and Rao, M. S. (1997). Isolation of lineage-restricted neuronal precursors from multipotent neuroepithelial stem cells. *Neuron* **19,** 773–785.

Mayer-Proschel, M., Liu, Y., Xue, H., Wu, Y., Carpenter, M., and Rao, M. S. (2002). Human neural precursor cells-Culture and in vitro characterization. *J. Clin. Neurosci.* **2,** 58–69.

McLaren, F. H., Svendsen, C. N., Van der Meide, P., and Joly, E. (2001). Analysis of neural stem cells by flow cytometry: Cellular differentiation modifies patterns of MHC expression. *J. Neuroimmunol.* **112,** 35–46.

Meeker, A. K., and Coffey, D. S. (1997). Telomerase: A promising marker of biological immortality of germ, stem, and cancer cells. A review. *Biochemistry (Mosc.)* **62,** 1323–1331.

Misumi, Y., and Kawano, H. (1998). The expressions of epidermal growth factor receptor mRNA and protein gene product 9.5 in developing rat brain. *Brain Res. Dev. Brain Res.* **107,** 1–9.

Moretto, G., Xu, R. Y., and Kim, S. U. (1993). CD44 expression in human astrocytes and oligodendrocytes in culture. *J. Neuropathol. Exp. Neurol.* **52,** 419–423.

Mujtaba, T., Piper, D. R., Kalyani, A., Groves, A. K., Lucero, M. T., and Rao, M. S. (1999). Lineage-restricted neural precursors can be isolated from both the mouse neural tube and cultured ES cells. *Dev. Biol.* **214,** 113–127.

Namiki, J., and Tator, C. H. (1999). Cell proliferation and Nestin expression in the ependyma of the adult rat spinal cord after injury. *J. Neuropathol. Exp. Neurol.* **58,** 489–498.

Nguyen, L., Rigo, J. M., Rocher, V., Belachew, S., Malgrange, B., Rogister, B., Leprince, P., and Moonen, G. (2001). Neurotransmitters as early signals for central nervous system development. *Cell Tissue Res.* **305,** 187–202.

Nieto-Sampedro, M., Gomez-Pinilla, F., Knauer, D. J., and Broderick, J. T. (1988). Epidermal growth factor receptor immunoreactivity in rat brain astrocytes. Response to injury. *Neurosci. Lett.* **91,** 276–282.

Okano, H. J., Pfaff, D. W., and Gibbs, R. B. (1996). Expression of EGFR-, p75NGFR-, and PSTAIR (cdc2)-like immunoreactivity by proliferating cells in the adult rat hippocampal formation and forebrain. *Dev. Neurosci.* **18,** 199–209.

Ostenfeld, T., Caldwell, M. A., Prowse, K. R., Linskens, M. H., Jauniaux, E., and Svendsen, C. N. (2000). Human neural precursor cells express low levels of telomerase in vitro and show diminishing cell proliferation with extensive axonal outgrowth following transplantation. *Exp. Neurol.* **164,** 215–226.

Panicker, M., and Rao, M. S. (2000). Stem cells in the nervous system. In "Stem Cells" (D. R. Marshak, R. L. Gardner, and D. Gottlieb, Eds.), pp. 399–438. Cold Spring Harbor Laboratory Press, Cold Spring Harbor, NY.

Pende, M., Holtzclaw, L. A., Curtis, J. L., Russell, J. T., and Gallo, V. (1994). Glutamate regulates intracellular calcium and gene expression in oligodendrocyte progenitors through the activation of DL-alpha-amino-3-hydroxy-5-methyl-4-isoxazolepropionic acid receptors. *Proc. Natl. Acad. Sci. USA* **91,** 3215–3219.

Piper, D. J., Mujtaba, J., Keyoung, H., Roy, N. S., Goldman, S. A., Rao, M. S., and Lucero, M. (2001). Identification and characterization of neuron restricted precursors and their progeny from human fetal tissue. *J. Neurosci. Res.* **66,** 356–68.

Pringle, N. P., Guthrie, S., Lumsden, A., and Richardson, W. D. (1998). Dorsal spinal cord neuroepithelium generates astrocytes but not oligodendrocytes. *Neuron* **20,** 883–893.

Pringle, N. P., Mudhar, H. S., Collarini, E. J., and Richardson, W. D. (1992). PDGF receptors in the rat CNS: During late neurogenesis, PDGF alpha-receptor expression appears to be restricted to glial cells of the oligodendrocyte lineage. *Development* **115,** 535–551.

Pringle, N. P., and Richardson, W. D. (1993). A singularity of PDGF alpha-receptor expression in the dorsoventral axis of the neural tube may define the origin of the oligodendrocyte lineage. *Development* **117,** 525–533.

Radley, J. M., Ellis, S., Palatsides, M., Williams, B., and Bertoncello, I. (1999). Ultrastructure of primitive hematopoietic stem cells isolated using probes of functional status. *Exp. Hematol.* **27,** 365–369.

Rao, M. S. (1999). Multipotent and restricted precursors in the central nervous system. *Anat. Rec.* **257,** 137–148.

Rao, M. S., and Mayer-Proschel, M. (1997). Glial-restricted precursors are derived from multipotent neuroepithelial stem cells. *Dev. Biol.* **188,** 48–63.

Rao, M. S., Noble, M., and Mayer-Proschel, M. (1998). A tripotential glial precursor cell is present in the developing spinal cord. *Proc. Natl. Acad. Sci. USA* **95,** 3996–4001.

Rasmussen, T., Bjorkstrand, B., Andersen, H., Gaarsdal, E., and Johnsen, H. E. (2002). Efficacy and safety of CD34-selected and CD19-depleted autografting in multiple myeloma patients: A pilot study. *Exp. Hematol.* **30,** 82–88.

Reynolds, B. A., Tetzlaff, W., and Weiss, S. (1992). A multipotent EGF-responsive striatal embryonic progenitor cell produces neurons and astrocytes. *J. Neurosci.* **12,** 4565–4574.

Reynolds, B. A., and Weiss, S. (1996). Clonal and population analyses demonstrate that an EGF-responsive mammalian embryonic CNS precursor is a stem cell. *Dev. Biol.* **175,** 1–13.

Rietze, R. L., Valcanis, H., Brooker, G. F., Thomas, T., Voss, A. K., and Bartlett, P. F. (2001). Purification of a pluripotent neural stem cell from the adult mouse brain. *Nature* **412,** 736–739.

Rozental, R., Srinivas, M., Gokhan, S., Urban, M., Dermietzel, R., Kessler, J. A., Spray, D. C., and Mehler, M. F. (2000). Temporal expression of neuronal connexins during hippocampal ontogeny. *Brain Res. Rev.* **32,** 57–71.

Sanchez-Gomez, M. V., and Matute, C. (1999). AMPA and kainate receptors each mediate excitotoxicity in oligodendroglial cultures. *Neurobiol. Dis.* **6,** 475–485.

Santa-Olalla, J., and Covarrubias, L. (1995). Epidermal growth factor (EGF), transforming growth factor-alpha (TGF-alpha), and basic fibroblast growth factor (bFGF) differentially influence neural precursor cells of mouse embryonic mesencephalon. *J. Neurosci. Res.* **42,** 172–183.

Scharenberg, C. W., Harkey, M. A., and Torok-Storb, B. (2002). The ABCG2 transporter is an efficient Hoechst 33342 efflux pump and is preferentially expressed by immature human hematopoietic progenitors. *Blood* **99,** 507–512.

Takahashi, T., Goto, T., Miyama, S., Nowakowski, R. S., and Caviness, V. S., Jr. (1999). Sequence of neuron origin and neocortical laminar fate: Relation to cell cycle of origin in the developing murine cerebral wall. *J. Neurosci.* **19,** 10357–10371.

Takahashi, T., Nowakowski, R. S., and Caviness, V. S., Jr. (1995). The cell cycle of the pseudostratified ventricular epithelium of the embryonic murine cerebral wall. *J. Neurosci.* **15,** 6046–6057.

Takano, T., and Becker, L. E. (1997). Developmental change of the Nestin-immunoreactive midline raphe glial structure in human brainstem and spinal cord. *Dev. Neurosci.* **19,** 202–209.

Thisse, B., Thisse, C., and Weston, J. A. (1995). Novel FGF receptor (Z-FGFR4) is dynamically expressed in mesoderm and neurectoderm during early zebrafish embryogenesis. *Dev. Dyn.* **203,** 377–391.

Tropepe, V., Sibilia, M., Ciruna, B. G., Rossant, J., Wagner, E. F., and Van der Kooy, D. (1999). Distinct neural stem cells proliferate in response to EGF and FGF in the developing mouse telencephalon. *Dev. Biol.* **208,** 166–188.

Van Raay, T. J., Wang, Y. K., Stark, M. R., Rasmussen, J. T., Francke, U., Vetter, M. L., and Rao, M. S. (2001). Frizzled 9 is expressed in neural precursor cells in the developing neural tube. *Dev. Genes Evol.* **211,** 453–457.

Wang, Y. K., Sporle, R., Paperna, T., Schughart, K., and Francke, U. (1999). Characterization and expression pattern of the frizzled gene Fzd9, the mouse homolog of FZD9 which is deleted in Williams-Beuren syndrome. *Genomics* **57,** 235–248.

Waschek, J. A., Dicicco-Bloom, E. M., Lelievre, V., Zhou, X., and Hu, Z. (2000). PACAP action in nervous system development,

regeneration, and neuroblastoma cell proliferation. *Ann. N. Y. Acad. Sci.* **921,** 129–136.

Weigmann, A., Corbeil, D., Hellwig, A., Huttner, and W. B. (1997). Prominin, a novel microvilli-specific polytopic membrane protein of the apical surface of epithelial cells, is targeted to plasmalemmal protrusions of non-epithelial cells. *Proc. Natl. Acad. Sci. USA* **94,** 12425–12430.

Weinrich, S. L., Pruzan, R., Ma, L., Ouellette, M., Tesmer, V. M., Holt, S. E., Bodnar, A. G., Lichtsteiner, S., Kim, N. W., Trager, J. B., Taylor, R. D., Carlos, R., Andrews, W. H., Wright, W. E., Shay, J. W., Harley, C. B., and Morin, G. B. (1997). Reconstitution of human telomerase with the template RNA component hTR and the catalytic protein subunit hTRT. *Nat. Genet.* **17,** 498–502.

Williams, B. P., Park, J. K., Alberta, J. A., Muhlebach, S. G., Hwang, G. Y., Roberts, T. M., and Stiles, C. D. (1997). A PDGF-regulated immediate early gene response initiates neuronal differentiation in ventricular zone progenitor cells. *Neuron* **18,** 553–562.

Wu, Y. Y., Mujtaba, T., and Rao, M. S. (2002). Isolation of stem and precursor cells from fetal tissue. *Methods Mol. Biol.* **198,** 29–40.

Yang, X., Handler, M., and Shen, J. (2000). Role of presenilin-1 in murine neural development. *Ann. N. Y. Acad. Sci.* **920,** 165–170.

Zhong, W., Jiang, M. M., Weinmaster, G., Jan, L. Y., and Jan, Y. N. (1997). Differential expression of mammalian Numb, Numblike and Notch1 suggests distinct roles during mouse cortical neurogenesis. *Development* **124,** 1887–1897.

Zimmerman, L., Parr, B., Lendahl, U., Cunningham, M., McKay, R., Gavin, B., Mann, J., Vassileva, G., and McMahon, A. (1994). Independent regulatory elements in the Nestin gene direct transgene expression to neural stem cells or muscle precursors. *Neuron* **12,** 11–24.

Received for publication March 6, 2002
Revised July 25, 2002
Accepted August 20, 2002
Published online October 15, 2002